

Competitive Non-Clairvoyant KV-Cache Scheduling for LLM Inference

Yiding Feng

Hong Kong University of Science and Technology, China, ydfeng@ust.hk

Zonghan Yang

Shanghai Jiao Tong University, China, fstqwq@sjtu.edu.cn

Yuhao Zhang

Shanghai Jiao Tong University, China, zhang_yuhao@sjtu.edu.cn

Abstract. Large Language Model (LLM) inference presents a unique scheduling challenge due to the Key-Value (KV) cache, where a job's memory footprint grows linearly with the number of decoded tokens. This growth couples scheduling decisions with feasibility: a scheduler must minimize latency under a hard memory budget, yet the response lengths of requests are inherently unknown. While recent works have explored this problem either assuming clairvoyance—exact knowledge of response lengths—or relying on machine-learned predictions, obtaining robust performance guarantees without any prior knowledge of job sizes remains a theoretically fundamental and practically important open problem.

In this work, we propose the Geometric Slicing Algorithm (GSA), the non-clairvoyant policy to achieve *the first constant competitive ratio for this problem in the offline batch setting*. GSA manages uncertainty through a geometric phase structure that periodically restarts jobs to bound memory exposure, combined with a staggered pipeline mechanism that enables high concurrency by smoothing aggregate memory consumption. We prove that GSA achieves a competitive ratio of at most 61.92 for general instances, improving to 32 in the large-memory regime. Our algorithmic framework also yields a clairvoyant counterpart, the Geometric Batching Algorithm (GBA), which achieves an approximation ratio of 10.67 for general instances and 6.75 in the large-memory regime—significantly improving upon the best previously known bound of over 9000. Numerical experiments on real request traces demonstrate that our algorithms perform robustly while preserving these worst-case guarantees.

Key words: KV-cache, non-clairvoyant scheduling, approximation algorithm, combinatorial optimization

1. Introduction

Large Language Models (LLMs) have emerged as the cornerstone of modern AI, powering chat assistants, search engines, and developer tools (Brown et al., 2020; OpenAI, 2023; Microsoft, 2023; Google, 2024b). While training remains a massive undertaking, the inference phase increasingly dominates operational costs—a trend amplified by the rise of reasoning-enhanced models that trade extensive Chain-of-Thought computation for improved capabilities (Wei et al., 2022; Jaech et al., 2024; Guo et al., 2025). These escalating resource demands strain deployment infrastructure significantly, impacting not only capital expenditures but also environmental sustainability (Strubell et al., 2019; Luccioni et al., 2024; Li et al., 2025a). Consequently, optimizing system efficiency without compromising quality-of-service requirements—such as latency—has become an operational imperative.

Virtually all foundation LLMs are built upon the Transformer architecture (Vaswani et al., 2017), whose self-attention mechanism computes dependencies across input tokens. To avoid quadratic recomputation at each decoding step, modern inference systems universally employ a *Key-Value (KV) cache* to store intermediate attention states (Kwon et al., 2023; Zheng et al., 2024b; Hooper et al., 2024). While this optimization reduces computational complexity to linear time, it introduces a critical resource trade-off: execution progress becomes tightly coupled with GPU memory consumption. This coupling has shifted attention toward systems-level optimization, especially KV-cache management.

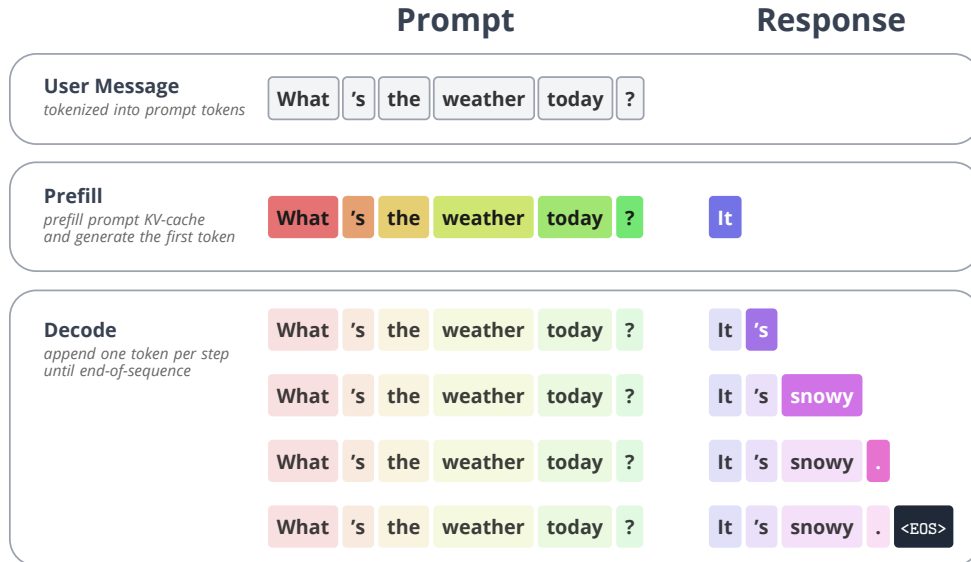


Figure 1 The diagram illustrates the LLM inference process flowing from top to bottom. First, the user message is tokenized. Next, the *prefill* phase processes the prompt to generate the first decode token. Then, the *decode* phase generates output tokens auto-regressively until the End-Of-Sequence token. Note that the KV-cache (colored context) grows linearly with each step.

As illustrated in Figure 1, when a user request arrives, it is tokenized and processed by the LLM in two phases. The *decode* phase then produces subsequent tokens auto-regressively, appending a new KV pair to the cache for each generated token. Consequently, the memory footprint of a request is *not static* but grows linearly with its response length.

This dynamic memory growth—where a request’s memory footprint increases linearly with its accumulated processing time—introduces a first fundamental challenge for LLM inference scheduling: *temporal coupling between concurrency and feasibility*. Unlike classical scheduling models that assume static resource requirements, the KV cache in LLMs expands as decoding progresses. Consequently, a batch of jobs that fits within memory at the start of execution may inevitably violate memory constraints later. This forces the scheduler to balance high concurrency against the risk of memory overflows, which trigger costly preemptions under kill-and-restart semantics—the core tension in efficient LLM serving.

Compounding this issue is a second critical challenge: *non-clairvoyance*. Because termination is governed by model-generated stop conditions rather than an externally specified job size, the final response length is not determined a priori and only gradually reveals itself during execution.¹ This uncertainty renders the processing time of each job unpredictable until completion, placing the problem squarely in the non-clairvoyant setting of classical scheduling theory. The lack of foresight harms average latency, as traditional clairvoyant strategies become brittle. Moreover, because the KV cache grows dynamically with generated tokens, uncertainty in response length directly translates into uncertainty in future memory footprints—a difficulty absent in classical models. Thus, the scheduler must simultaneously manage both temporal resource coupling and incomplete information, navigating a doubly constrained trade-off between latency and memory safety.

Motivated by these challenges and the critical importance of efficient LLM inference scheduling, we ask:

Can we design effective batching policies for LLM inference requests that remain robust to the risk of infeasibility caused by dynamic memory growth, even in non-clairvoyant environments?

To address this question, we adopt the offline batch scheduling model studied in recent literature (e.g., Jaillet et al., 2025; Wang et al., 2025; Chen et al., 2025). In this model, all inference requests arrive simultaneously at time zero and are processed on a single GPU under a hard KV-cache memory budget. Each request consists of a fixed-length prompt followed by an unknown number of output tokens (i.e., response length) generated autoregressively, creating a non-clairvoyant environment. Since our focus is exclusively on scheduling the decode phase, the prefill phase—which initializes the KV cache from the prompt and

¹ Some practical systems introduce response-length predictors to inform batching, admission control, or memory reservation. However, these predictors provide only noisy, workload-dependent estimates rather than oracle knowledge, and they lack guarantees that would eliminate non-clairvoyance (Zheng et al., 2023; Jin et al., 2023; Fu et al., 2024). This direction has been explored in recent prior work (Chen et al., 2025). See more discussion in related work (Section 1.3).

generates the first token—is assumed to be completed in a single time step (i.e., the duration of decoding one token)².

During decoding, a request’s memory footprint grows linearly with its progress: each generated token appends to the KV cache, increasing total memory consumption. At every round, the scheduler must decide which subset of unfinished requests to process as a batch on the GPU. If executing the chosen batch would violate the memory budget, the scheduler is forced to preempt (i.e., kill) some currently active requests, discarding all their partial progress, which reflects the prohibitive cost of state swapping in real systems. Critically, the scheduler operates in a non-clairvoyant setting: it does not know how long each request will run until it completes.

The objective is to minimize *total flow time*, i.e., the sum of job completion times, which directly captures end-to-end latency in the offline batch setting. We evaluate non-clairvoyant algorithms via their *competitive ratio*: the worst-case ratio of their total flow time to that of an optimal clairvoyant scheduler with full knowledge of all response lengths. For completeness, we also analyze the clairvoyant counterpart of our algorithm, which serves as a structural proxy in our competitive analysis.

1.1. Our Contributions

In this paper, we provide compelling answers to the questions posed above. In a nutshell, we present the *first $O(1)$ -competitive algorithm* for the non-clairvoyant offline batch scheduling model under dynamic KV-cache memory constraints, without any assumptions on the input instance. Moreover, under the practically relevant *large-memory regime*, where the KV-cache budget is sufficiently large relative to prompt and response lengths,³ we obtain an improved competitive ratio. More formally, our first main result is as follows:

Main Result (I) *We propose a non-clairvoyant, polynomial-time scheduling algorithm (Algorithm 2). For general instances, it achieves a competitive ratio of at most 61.92; for large-memory instances, this improves to 32.*

Our algorithmic framework also yields better guarantees in the clairvoyant setting. In particular, we show that a natural clairvoyant counterpart of our algorithm—designed with full knowledge of request response lengths—yields even stronger guarantees, significantly improve upon previous results. Formally, our second main result is:

² This assumption is justified as practical systems often handle the prefill phase separately via prefill/decode disaggregation (Zhong et al., 2024; Choukse et al., 2025).

³ The large-memory assumption is well-motivated in LLM inference and cloud computing settings, and is commonly adopted in prior work on LLM scheduling and online resource allocation (see, e.g., Kalyanasundaram and Pruhs, 2000; Mehta et al., 2007; Golrezaei et al., 2014; Ma and Simchi-Levi, 2020; Chen et al., 2025).

Table 1 Summary of results and comparison with prior work

	Setting	This Work	Prior Work
Non-Clairvoyant	General Instances	61.92 (Theorem. 2)	(unknown)
	Large-Memory Instances	32 (Theorem. 2)	$O(\log M)$ (Chen et al., 2025)
Clairvoyant	General Instances	10.67 (Theorem. 3)	9216 (Jaillet et al., 2025)
	Large-Memory Instances	6.75 (Theorem. 3)	48 [‡] (Wang et al., 2025)
Clairvoyant Identical Jobs	General Instances	2 (Theorem. 1)	4 (Jaillet et al., 2025)
	Large-Memory Instances	1[†] (Theorem. 1)	4 (Jaillet et al., 2025)

Note: Numbers represent competitive ratios (for non-clairvoyant algorithms) and approximation ratios (for clairvoyant algorithms). All large-memory instances assume that the KV-cache memory budget $M \rightarrow \infty$ while the prompt lengths and response lengths remain fixed. [†] additionally requires the number of jobs $n \rightarrow \infty$. [‡] continues to hold even under heterogeneous prompt lengths (Wang et al., 2025).

Main Result (II) We propose a clairvoyant, polynomial-time scheduling algorithm (Algorithm 3), which serves as the structural analog of Algorithm 2. For general instances, it achieves an approximation ratio of at most 10.67; for large-memory instances, this improves to 6.75. When all requests have identical response lengths, the ratio further improves to 2 in general and asymptotically approaches 1 in the large-memory limit.

We summarize all our results and compare them with prior work in Table 1. Although LLM inference and its optimization under KV-cache constraints are relatively recent, there has been a rapidly growing algorithmic literature on scheduling for this setting. Among the various models studied, the offline batch scheduling model—which we adopt—is one of the most prominent due to its practical relevance and mathematical tractability.

In the non-clairvoyant setting, Chen et al. (2025) proposed a scheduling policy whose analysis is tailored to the large-memory instances (where the memory capacity $M \rightarrow \infty$). They establish the first bounded competitive ratio of $O(\log M)$. In contrast, as our first main result, we present the first constant-competitive algorithm for general instances, achieving a competitive ratio of at most 61.92 without any asymptotic assumptions.⁴

⁴ In Section 1.2 and Section 3.2, we explain why constant competitiveness cannot be achieved by certain classic heuristics—including the algorithm of Chen et al. (2025) and how it motivates one key algorithmic ingredient in our algorithm.

For the clairvoyant setting, constant-approximation algorithms have been previously designed. [Jaillet et al. \(2025\)](#) propose a clairvoyant scheduler and prove an approximation ratio of 9216.⁵ For large-memory instances, this was later improved to 48 by [Wang et al. \(2025\)](#).⁶ Our second main result—a clairvoyant structural analog of our non-clairvoyant algorithm—significantly improves these guarantees: we reduce the approximation ratio from 9216 to 10.67 for general instances and from 48 to 6.75 for large-memory instances.⁷

We further validate our theoretical insights through numerical experiments (Section [EC.1](#)). Using both synthetic workloads and real-world traces from the LMSYS-Chat-1M dataset, we observe that the structural properties of our geometric scheduling framework—such as staggered execution and disciplined phase-based preemption—can lead to meaningful practical improvements. In our evaluations, our algorithms perform favorably against state-of-the-art baselines across a range of settings, and heuristic variants (GBA-D and GSA-SPEC) demonstrate robust behavior while preserving worst-case guarantees.

1.2. Overview of the Techniques

As discussed above, we develop a unified algorithmic framework that achieves strong performance guarantees in both non-clairvoyant and clairvoyant settings. Realizing this goal requires overcoming four key challenges: (i) maintaining batching feasibility effectively under dynamic KV-cache memory constraints; (ii) handling heterogeneity in request response lengths; (iii) coping with uncertainty about response lengths (i.e., non-clairvoyance); and (iv) analyzing performance against an optimal clairvoyant scheduler that is difficult to characterize explicitly.

Challenges (i) and (ii) arise in both clairvoyant and non-clairvoyant settings, but are exacerbated by challenge (iii)—the lack of knowledge about request sizes—which makes effective batching significantly harder. Challenge (iv) is primarily analytical: because the optimal clairvoyant schedule has no simple closed form, standard competitive or approximation analysis techniques do not apply directly.

Our framework combines two key ingredients: *staggered pipelining* and *geometric slicing*. Staggered pipelining tackles challenge (i) by enabling high concurrency under dynamic memory constraints. Geometric slicing addresses challenges (ii) and (iii) by grouping jobs into geometrically spaced classes based on estimated response lengths, balancing load and remaining robust to estimation errors.

To handle the analytical difficulty of challenge (iv), we introduce a novel *memory-time area* perspective. This geometric view yields a tractable bound on the optimal clairvoyant scheduler and provides a common metric to compare our algorithms against the optimum—effectively bridging scheduling decisions and resource consumption for competitive and approximation analyses.

⁵ While [Jaillet et al. \(2025\)](#) state their result as an $O(1)$ approximation (Theorem 4.3), the explicit constant 9216 arises from combining multiplicative factors in their structural lemmas (1536 from Lemma 4.4 and 6 from Lemma 4.7).

⁶ [Wang et al. \(2025\)](#) establishes the approximation ratio of 48 even under heterogeneous prompt lengths.

⁷ In Section [1.2](#) and Section [3.1](#), we detail how our staggered pipeline design enables smoother memory usage and higher concurrency, which eventually translates into tighter approximation bounds.

Below, we discuss each of these components and their integration into our algorithms in greater detail.

Smoothing Memory Footprints via Staggered Pipeline. A common approach used in both standard heuristics (e.g., First-Come-First-Served or Shortest-Job-First) and policies in prior work (e.g., Kwon et al., 2023; Zheng et al., 2024a; Jaillet et al., 2025; Chen et al., 2025) is *simultaneous batching*: packing as many requests as possible into a single batch and executing them in lockstep. This strategy is well-motivated in the classic flow-time minimization setting (where memory consumption is static) and is indeed optimal for identical requests under that model. However, simultaneous batching is inherently memory-inefficient in the KV-cache setting. Because all requests in a batch progress through decoding at the same rate, they reach their peak memory usage simultaneously. To avoid overflow, the scheduler must restrict the batch size based on this collective peak, resulting in a “sawtooth” memory profile where a significant portion of the memory budget remains underutilized on average.

Motivated by this inefficiency, we propose STAGGERED-PIPELINE-SCHEDULE (SPS), a core scheduling subroutine that forms the foundation of our main algorithms. Despite its simplicity, SPS *provides a principled approach to smoothing memory footprint over time, thereby enabling significantly higher concurrency under a fixed memory budget*. As such, it may be of independent interest for broader memory-constrained scheduling problems.

More precisely, SPS is designed to process a set of requests with identical response lengths—or, more generally, a fixed time slice, where any request not completed within its allotted slice is killed. Rather than starting all requests simultaneously, SPS intentionally offsets their start times to “smooth out” aggregate memory consumption. By staggering execution so that different requests reach their peak memory usage at distinct rounds, SPS sustains a much higher degree of concurrency within the same memory budget.

Visual comparison between SPS and simultaneous batching is provided in Example 1, Figure 2, and Figure EC.1. Thanks to its higher concurrency, SPS achieves a better approximation ratio even for identical requests, and is asymptotically optimal in the large-memory regime. When combined with our other algorithmic ingredients, this improvement translates directly into stronger guarantees for more general settings.

Kill Two Birds with One Stone: Geometric Slicing for Effective Grouping. While SPS enables high concurrency for requests with identical response lengths, it does not address heterogeneity in response lengths or the uncertainty inherent in the non-clairvoyant setting. We resolve both challenges with a single idea: *geometric slicing*, which groups requests into geometrically spaced classes based on their true response lengths (in the clairvoyant setting) or estimated lengths (in the non-clairvoyant setting).

We first describe the clairvoyant case, which is simpler. Our algorithm GEOMETRIC-BATCHING-ALGORITHM (GBA, see Algorithm 3) is parameterized by a scaling factor $\alpha \in (1, \infty)$. It partitions all requests into classes $p = 0, 1, \dots$ according to geometrically increasing time scales:

$$\widehat{\tau}_p = \alpha^p \cdot \widehat{\tau}_0,$$

where $1 \leq \hat{\tau}_0 \leq \alpha$ is an initial time slice. For each class p , GEOMETRIC-BATCHING-ALGORITHM invokes SPS with time slice $\lceil \hat{\tau}_p \rceil$, which—by construction—is sufficient to complete all class- p requests. As in classical flow-time minimization, processing shorter requests first improves total flow time; invoking SPS per class ensures high concurrency while respecting the KV-cache memory constraint.

Our non-clairvoyant algorithm GEOMETRIC-SLICING-ALGORITHM (GSA, see Algorithm 2) follows the same geometric structure. It uses the same parameters α and $\hat{\tau}_0$, and executes SPS with time slice $\lceil \hat{\tau}_p \rceil$ in phase p . The key difference is that, without knowledge of true response lengths, it cannot isolate class- p requests. Instead, it runs SPS on all remaining (unfinished) requests in each phase. Although this introduces overhead compared to the clairvoyant counterpart, our analysis shows this overhead is tightly controlled.

In fact, the choice of α entails a fundamental tradeoff. A small α yields many fine-grained classes, which may contain too few requests to fully utilize SPS, thereby reducing concurrency. It also increases overhead in the non-clairvoyant setting, as GSA performs more frequent kill-and-restart operations across a larger number of phases. Conversely, a large α produces coarse classes where the allocated time slice significantly exceeds the actual response lengths of many requests, leading to wasted memory and compute resources. We optimize α for different regimes to achieve the competitive and approximation ratios reported in Table 1. In practice, both α and $\hat{\tau}_0$ are tunable parameters (see Section EC.1 for further discussion).

It is also worth highlighting that GSA employs a counter-intuitive *aggressive preemption* strategy: it systematically terminates all unfinished requests at the end of each phase. This contrasts sharply with many heuristics and policies in prior work, which avoid preemption unless the memory budget is exceeded—aiming to minimize restarts and associated wasted computation. Moreover, when preemption is unavoidable, those approaches typically prefer killing requests with shorter processing times. While intuitive, this strategy can severely degrade performance under the flow-time objective: long-running requests block memory for extended periods, limiting parallelism and inflating total flow time. As illustrated in Example 2, this distinction is crucial—GSA’s disciplined phase-based preemption enables it to outperform such heuristics by maintaining higher concurrency and smoother memory utilization.

Competitive/Approximation Analysis via the Memory-Time Area Perspective. A central challenge in our analysis is the intractability of the optimal scheduler. Due to the dynamic memory footprint and the hard KV-cache constraint, the optimal schedule can be highly complex. While it can be formulated as an integer program—and some prior work (e.g., [Jaillet et al., 2025](#)) uses its linear programming relaxation and dual as a performance upper bound—this approach remains technically cumbersome.

In contrast, we take a fundamentally different approach based on *memory-time area*, which is defined as the total KV-cache resources consumed by a request over its execution, combining fixed prompt memory and linearly growing decode cache (see Definition 1 and the colored triangles/trapezoids in Figure 2).

This perspective yields a clean accounting principle: any feasible schedule’s total memory-time area cannot exceed the area supplied by the memory budget over time. Crucially, this enables two insights. First,

under the relaxed constraint that only total area must be respected (a necessary condition for feasibility), the optimal schedule becomes simple: process jobs in non-decreasing order of response length. This provides a tractable upper bound on the true optimum.

Second, the area view allows us to precisely quantify the packing efficiency of SPS. We show that both the clairvoyant GBA (which applies SPS per class) and SPS itself achieve approximately optimal area utilization, directly yielding strong approximation guarantees. Finally, leveraging the structural similarity between GSA and GBA, we bound the non-clairvoyant overhead by a constant factor, establishing GSA’s constant competitive ratio.

1.3. Further Related Work

We further review related work in the theoretical literature that provides foundational techniques for our algorithmic framework.

Packing Problems. The offline batch scheduling problem under KV-cache constraints shares structural similarities with two-dimensional packing. In our memory-time area framework, jobs occupy triangular or trapezoidal footprints, and scheduling them within the memory budget resembles packing shapes into a strip of fixed width. [Lodi et al. \(2002\)](#) provide a comprehensive survey of 2D orthogonal packing variants (e.g., bin packing and strip packing for rectangles), summarizing the complexity landscape and standard algorithmic paradigms including exact methods, approximation algorithms, and heuristics. For strip packing specifically, [Adamaszek et al. \(2017\)](#) prove APX-hardness with polynomially bounded item dimensions—in particular, it is NP-hard to approximate within a factor better than $12/11 - \varepsilon$.

Flow Time Minimization. Minimizing total flow time on parallel machines has been extensively studied. [Leonardi and Raz \(2007\)](#) develop approximation algorithms for total flow time on parallel machines with release dates, providing the first nontrivial approximation guarantees for this setting. [Awerbuch et al. \(2002\)](#) study flow-time minimization under the restriction that jobs cannot migrate between machines, providing competitive guarantees via techniques that compare to migratory benchmarks. More recently, [Geng et al. \(2025\)](#) establish tight randomized bounds for online non-preemptive total flow time on identical machines, matching $\Theta(\sqrt{n/m})$ upper and lower bounds, and extend the framework to kill-and-restart preemption with similar bounds.

Non-Clairvoyant Scheduling. The non-clairvoyant scheduling model, where processing times are revealed only upon job completion, was formalized by [Motwani et al. \(1994\)](#), who prove foundational upper and lower bounds and analyze baseline policies including round-robin for flow-time objectives. [Becchetti and Leonardi \(2001\)](#) analyze non-clairvoyant flow-time minimization on single and parallel machines, showing competitiveness of multilevel-feedback-style randomized strategies under adversarial models. These classical results assume costless preemption: a job can be paused and resumed without penalty. In contrast, [Jäger](#)

et al. (2025) study non-clairvoyant single-machine scheduling with kill-and-restart preemption, where preempted jobs lose all progress, proving lower bounds for deterministic strategies and giving tight analyses for scaling restart strategies.

Scheduling with Partial Information. Between the extremes of clairvoyance and non-clairvoyance, several intermediate information models have been studied. Bechetti et al. (2004) formalize semi-clairvoyant scheduling where only coarse size classes are known, deriving constant-competitive algorithms for average flow time. Azar et al. (2022) develop online single-machine flow-time algorithms that remain competitive for every distortion level between predicted and true processing times. Im et al. (2023) introduce prediction-augmented non-clairvoyant scheduling for minimizing total completion time, designing algorithms with robustness-consistency guarantees as prediction error varies. Benomar and Perchet (2024) study non-clairvoyant scheduling where predictions are available for only a subset of jobs, establishing near-optimal bounds and a learning-augmented algorithm with robustness-consistency-smoothness tradeoffs. Benomar et al. (2025) study non-clairvoyant scheduling with continuous feedback in the form of progress estimates, providing competitive algorithms under adversarial and stochastic progress-bar models.

Scheduling for LLM Inference. Jaillet et al. (2025) formalize online batching under a hard KV-cache memory constraint, establish strong impossibility results for adversarial arrivals, and propose a greedy shortest-first policy with bounded competitive guarantees under restricted assumptions. Wang et al. (2025) study settings with heterogeneous prefill and decode lengths, prove that the resulting batching problem is NP-hard, and design constant-competitive schedulers. Chen et al. (2025) consider the same offline batch inference model as ours and propose a scheduling algorithm with an approximation ratio of $O(\log(o_{\max}/o_{\min}))$ in the large-memory regime, where o_{\max} and o_{\min} denote the maximum and minimum response lengths, respectively. Since $o_{\max} \leq M$ and $o_{\min} \geq 1$, their result implies a non-clairvoyant competitive ratio of $O(\log M)$ for large-memory instances. They also analyze algorithm performance under additional distributional assumptions on response lengths.

Beyond worst-case analysis, Ao et al. (2025) introduce a fluid approximation as an analytical benchmark and derive threshold-based online policies with heavy-traffic optimality guarantees. Li et al. (2025b) adopt a queueing-theoretic perspective, proving throughput-optimality for work-conserving policies in LLM serving. Zhang et al. (2025b) address prompt caching in multi-turn conversations, focusing on tail latency; they propose a modified LRU policy optimized for P90/P95 objectives.

2. Preliminaries

2.1. Model and Objective

We now establish the formal framework for the non-clairvoyant scheduling problem. While abstract, this model captures the operational realities of modern LLM inference; we refer the reader to Section 2.2 for detailed justifications of our core assumptions.

Jobs and Scheduling Actions. The system consists of a single computational worker (aka., a GPU) managed by a scheduler. There are n jobs (aka., inference requests), each job i has a *prompt* of length $s \in \mathbb{N}$ and a *response length* (aka., the number of decode tokens) $o_i \in \mathbb{N}$, which is the number of time units needed to complete the job once it starts. In this paper, we focus on the offline batch setting with identical prompt sizes, i.e., all jobs are available at time 0 and share a common prompt length s .

Time proceeds in discrete, unit-length rounds $t = 0, 1, 2, \dots$. Let $u_{i,t} \in \{0, \dots, o_i\}$ be the amount of processing the job has received up to the *start* of round t . If job i reaches $u_{i,t} = o_i$ at round t , then this job is completed (aka., finished) and its completion time is defined as t . At the beginning of each round t , the scheduler chooses an *active batch* $\mathcal{B}_t \subseteq [n]$ of unfinished jobs to process. During round t , every active job $i \in \mathcal{B}_t$ receives one unit of processing (i.e., decode the next token), so

$$u_{i,t+1} = u_{i,t} + 1.$$

The active batch is *dynamic*: its composition can change in each round. Essentially, the scheduler may perform two actions at the beginning of each round by choosing \mathcal{B}_t :

1. (Start): activate an inactive job $i \notin \mathcal{B}_{t-1}$ where $u_{i,t} = 0$.
2. (Kill): deactivate an active, unfinished job $i \in \mathcal{B}_{t-1} \setminus \mathcal{B}_t$ where $u_{i,t} < o_i$, discarding all its accumulated progress and resetting $u_{i,t+1}$ to 0.

KV-Cache Memory Feasibility. Unlike classical parallel scheduling with only a hard limit on the number of concurrent jobs, our model features a *KV-cache memory budget* $M \in \mathbb{N}$. This budget constrains the total memory used by active jobs, which grows as the tokens are decoded one by one. When job i has received $u_{i,t}$ units of processing by round t , it occupies $s + u_{i,t} + 1$ units of KV-cache memory: s units for the prompt and one additional unit for each decoded token (including the token being decoded in round t). Thus, the memory feasibility constraint requires

$$\forall t \in \mathbb{N}: \quad \sum_{i \in \mathcal{B}_t} (s + (u_{i,t} + 1)) \leq M. \quad (\text{MEMORY-FEASIBILITY})$$

To avoid trivial infeasibility, we assume *per-job feasibility*: $s + o_i \leq M$ for all jobs $i \in [n]$. This ensures that any job can be completed when processed in isolation.

Non-Clairvoyant Environment. Our base model assumes a *non-clairvoyant scheduler*, who does not know the response length o_i of any job i in advance. This value is revealed only upon the job's completion. In addition to the base model, we also consider a clairvoyant variant (in Section 4) in which the scheduler has full knowledge of all response lengths $\{o_i\}_{i \in [n]}$.

Objective and Benchmark. The scheduler’s objective is to minimize the *total flow time* (aka., end-to-end latency).⁸ Let ALG be a scheduling algorithm, and let c_i denote the round in which job i completes under ALG . The total flow time of ALG is defined as

$$\text{FLOWTIME}[\text{ALG}] \triangleq \sum_{i \in [n]} c_i.$$

Our primary focus is on designing non-clairvoyant algorithms that operate without knowledge of job sizes. To quantify the performance loss incurred by this lack of information, we benchmark our algorithms against OPT , the minimum total flow time achievable by any clairvoyant scheduler satisfying the memory feasibility constraint (**MEMORY-FEASIBILITY**). We use the standard terminology of *competitive ratio* for this comparison. Specifically, ALG is Γ -*competitive* if, for every problem instance, $\text{FLOWTIME}[\text{ALG}] \leq \Gamma \cdot \text{OPT}$.⁹ For clairvoyant algorithms where the comparison is against the optimal solution of the same information structure, this measure is referred to as the *approximation ratio*.

2.2. Discussion on the Model Primitives

We next explain several key modeling choices made in our problem formulation. Our theoretical model abstracts the complex dynamics of LLM inference systems. Here, we elaborate on the practical considerations that inform our theoretical abstractions and place our work in the context of related literature.

Offline Batch Inference and Identical Prompt Lengths. We assume all jobs are available at time 0 and share identical prompt lengths. This models the *offline batch inference* scenario, a common industry practice for high-throughput tasks where aggregating requests of similar prompt lengths is practical and cost-effective. For instance, both OpenAI and Google offer Batch APIs for processing large workloads asynchronously, often with significant cost savings (OpenAI, 2024; Google, 2024a). Our model can be viewed as optimizing the scheduling in every single batch request with similar prompt lengths. Furthermore, the identical prompt length assumption is also motivated by fixed prompt scenarios such as *agentic workflows*, where each agent is defined by a fixed system prompt and inference providers use prefix caching to reuse KV tensors corresponding to these prompts across iterations (Zhang et al., 2025a; He et al., 2025; Pan et al., 2025). Since the system prompts remain constant, the dominant part of prompt lengths becomes more uniform across requests.

Theoretically speaking, we introduce these two assumptions to isolate the algorithmic challenges arising from the growing memory scenario and the non-clairvoyant perspective. The rationale is that relaxing either assumption renders the problem significantly more difficult, even for clairvoyant schedulers with static memory:

⁸ In our setting, all jobs are available at time zero, so flow time equals completion time.

⁹ We allow the optimal clairvoyant scheduler to preempt or pause jobs (i.e., retain a job in memory without processing it). However, it can be shown that neither preemption nor pausing is necessary in an optimal solution, as postponing the start of a job will always be a better choice.

- (*Online arrivals*) Given identical prompt lengths, setting $s = M/2$ simplifies the problem to online single-machine scheduling to minimize total flow time under kill-and-restart preemption. This problem admits a competitive ratio lower bound of $\Omega(\sqrt{n})$ for n jobs, even for randomized algorithms (Epstein and van Stee, 2003).
- (*Heterogeneous prompt lengths*) In the offline batch setting where $o_i = 1$ for all jobs, allowing heterogeneous prompt lengths reduces the problem to Min-Sum Bin Packing, which is strongly NP-hard (Epstein et al., 2018).

Consequently, without these two assumptions, the analysis would deviate from our primary focus and become bogged down by the aforementioned fundamental hardness results.

Memory Model. The constraint (**MEMORY-FEASIBILITY**) assumes that memory is consumed strictly linearly with the number of decoded tokens and that fragmentation is negligible. This assumption is grounded in modern inference engine architectures, specifically the *PagedAttention* mechanism introduced in vLLM (Kwon et al., 2023), and also in other LLM inference systems (NVIDIA, 2023; Zheng et al., 2024b). *PagedAttention* partitions the KV-cache into fixed-size blocks that can be stored in non-contiguous memory, effectively eliminating external fragmentation. Consequently, the memory budget M represents the total number of available token slots (or blocks) on the GPU, and feasibility is determined solely by the total count of tokens, as modeled in (**MEMORY-FEASIBILITY**).

Modeling Prefill Cost via Kill-and-Restart. Although our model does not explicitly represent the prefill phase, its cost is implicitly captured by our kill-and-restart preemption mechanism. In modern LLM inference systems, the primary output of the prefill phase is the construction of the initial KV-cache for the prompt. When a request is preempted, this KV-cache state must either be swapped to slower memory or discarded entirely. In the latter case, resuming the request requires rerunning the prefill computation from scratch to reconstruct this state. Our model focuses on the kill-and-restart dynamic, as it cleanly captures the essential trade-offs in high-throughput systems. This modeling choice is grounded in the operational reality of inference engines, where the I/O overhead of swapping the KV-cache is often prohibitively expensive, making kill-based preemption the preferred strategy (Kwon et al., 2023).

Furthermore, the prefill phase can be of separate interest and can be addressed orthogonally. In practice, prefill can be handled by *prefill/decode disaggregation* (PD separation), which assigns prefill and decode to distinct resource pools. This architectural choice reduces phase interference and enables phase-specific optimizations (Zhong et al., 2024; Choukse et al., 2025). Accordingly, our model measures time in unit rounds corresponding to a single decode step (one output token) and does not explicitly include the prefill stage in the scheduling horizon.

3. Geometric Slicing Algorithm

Our main contribution is a non-clairvoyant KV-cache scheduling algorithm, GEOMETRIC-SLICING-ALGORITHM (GSA). In Section 3.1, we first introduce the STAGGERED-PIPELINE-SCHEDULE policy, which is near-optimal for instances with identical jobs. This policy serves as the core subroutine of GSA, which we present in Section 3.2 with all its algorithmic ingredients. The competitive ratio analysis of GSA is deferred to Sections 4 and 5.

3.1. Subroutine: STAGGERED-PIPELINE-SCHEDULE

In this section, we introduce STAGGERED-PIPELINE-SCHEDULE (SPS), a core scheduling subroutine that serves as the foundation for our main algorithms. While simple in its construction, SPS addresses a fundamental inefficiency in how current systems handle KV-cache memory, and its design may be of independent interest for broader memory-constrained scheduling problems.

The design of SPS is motivated by a canonical setting: *given a sequence of jobs \mathcal{J} with identical prompt length s and response length o , how can we schedule them to minimize total completion time (or equivalently, maximize throughput) under a fixed memory budget?*

The Simultaneous Batching Trap. A conventional approach to this problem is *simultaneous batching*: packing as many jobs as possible into a single batch and executing them in lockstep. This strategy is a natural consequence of standard policies like First-Come-First-Served (FCFS) or Shortest-First under certain conditions, and is widely adopted in LLM serving systems (Kwon et al., 2023; Zheng et al., 2024b) as well as the theoretical literature (Jaillet et al., 2025; Chen et al., 2025).¹⁰

However, simultaneous execution is inherently memory-inefficient. Since all jobs in a batch progress through their generation phases at the same rate, they reach their peak memory usage simultaneously. To prevent memory overflow, the scheduler must limit the batch size based on this collective peak. This leads to a “sawtooth” memory profile where, on average, a significant portion of the memory budget remains underutilized, as illustrated in Example 1 and Figure 2b.

SPS Subroutine: Smoothing via Staggering. To overcome this bottleneck, STAGGERED-PIPELINE-SCHEDULE (SPS) adopts a *staggered* execution strategy. Instead of starting all jobs at once, SPS intentionally offsets their start times to “smooth out” the aggregate memory consumption over time. By ensuring that different jobs reach their peak memory usage at different rounds, SPS can safely sustain a much higher degree of parallelism within the same memory budget.

Formally, SPS is parameterized by a *degree of parallelism* k and a *slice length* τ . For a sequence of jobs indexed $i = 0, \dots, |\mathcal{J}| - 1$, it schedules job i to start at round $t_i^{(\text{start})} \triangleq \lfloor i \cdot \tau / k \rfloor$. When the slice length τ is

¹⁰ Notably, in the classic flow-time minimization scheduling problem (where memory occupation remains static over time) with identical jobs, simultaneous batching is indeed optimal.

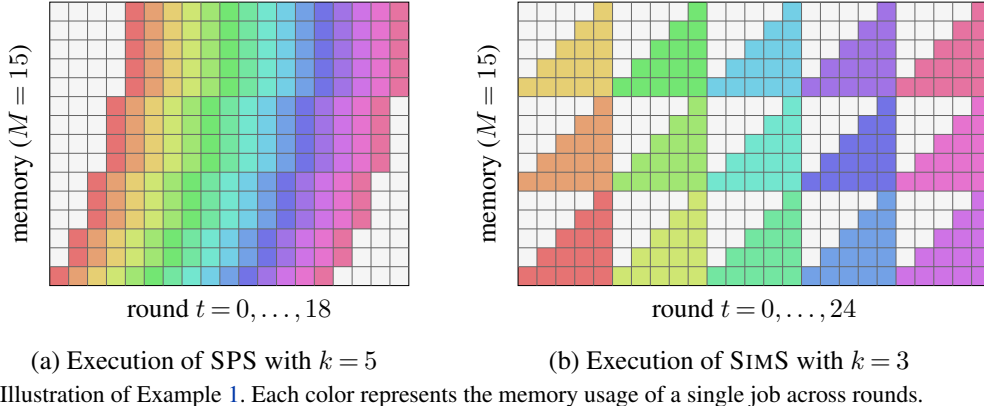


Figure 2 Illustration of Example 1. Each color represents the memory usage of a single job across rounds.

set to the identical response length o , each job completes at round $t_i^{(\text{end})} \triangleq t_i^{(\text{start})} + o$. A detailed description is provided in Procedure 1, and a visual comparison is shown in Example 1 and Figure 2a.

Procedure 1: STAGGERED-PIPELINE-SCHEDULE (SPS)

input : Sequence of jobs $\mathcal{J} = \{j_0, j_1, \dots\}$, Degree of parallelism $k \in \mathbb{N}$, Slice length $\tau \in \mathbb{N}$
output: Start time $t_i^{(\text{start})}$ and end time $t_i^{(\text{end})}$ for each job $j_i \in \mathcal{J}$

```

1 for each job index  $i \in \{0, 1, \dots, |\mathcal{J}| - 1\}$  do
2   set start time  $t_i^{(\text{start})} \leftarrow \lfloor i \cdot \tau / k \rfloor$ ;
3   set end time  $t_i^{(\text{end})} \leftarrow t_i^{(\text{start})} + \tau$ ;
4   schedule job  $j_i$  to run in the interval  $[t_i^{(\text{start})}, t_i^{(\text{end})})$ ;
   /* Jobs not completed by the start of round  $t_i^{(\text{end})}$  are killed. */
5 return  $\{t_i^{(\text{start})}, t_i^{(\text{end})}\}_{j_i \in \mathcal{J}}$ ;

```

EXAMPLE 1 (A TOY EXAMPLE WITH IDENTICAL JOBS). Consider an instance with 15 identical jobs (indexed $i = 0, \dots, 14$), each having prompt length $s = 0$ and response length $o = 5$, under a KV-cache memory budget of $M = 15$.

Under STAGGERED-PIPELINE-SCHEDULE (SPS) with degree of parallelism $k = 5$ and slice length $\tau = o = 5$, the i -th job starts at round $\lfloor 5i/5 \rfloor = i$. The last job ($i = 14$) starts at round 14 and completes at the end of round 18. This yields a total flow time of $\text{FLOWTIME[SPS]} = 5 + 6 + \dots + 19 = 180$. See Figure 2a for a graphical illustration.

In contrast, SIMULTANEOUS-SCHEDULE (SIMS) processes $k = 3$ jobs at a time, starting new jobs in rounds 0, 5, 10, 15, and 20. This yields a lower degree of parallelism due to peak memory constraints, and the last job finishes at round 25, resulting in a total flow time of $\text{FLOWTIME[SIMS]} = 225$. See Figure 2b for a graphical illustration.

Theoretical Guarantees of SPS. Through Example 1 and Figure 2, we observe that SPS achieves strong performance in this simple instance. Compared to SIMULTANEOUS-SCHEDULE, SPS exhibits significantly smoother memory usage over time, which in turn enables a higher degree of parallelism under the same memory budget. We now formalize these observations with the following theoretical guarantees for SPS.

THEOREM 1 (Approximation of SPS for Identical Jobs). *Let \mathcal{J} be a sequence of jobs with identical prompt length s and identical response length o . Then the schedule produced by STAGGEREDPIPELINESCHEDULE with a proper choice of parameters has an approximation ratio at most 2. Moreover, when prompt length s and response length o are fixed and both KV-cache memory budget $M \rightarrow \infty$ and the number of jobs $|\mathcal{J}| \rightarrow \infty$ with $M = o(|\mathcal{J}|)$, the approximation ratio converges to $1 + o(1)$.*

We remark that the above theorem guarantees both the asymptotic optimality of SPS and a worst-case approximation ratio of 2. In contrast, as shown in Section EC.2.2, SIMULTANEOUS-SCHEDULE incurs an approximation ratio of at least 2 even in this asymptotic regime.

In the following, we prove Theorem 1. We begin by establishing two key lemmas concerning the memory usage and the maximum feasible degree of parallelism in SPS.

LEMMA 1 (Peak Memory Usage of SPS). *For any sequence of jobs with identical prompt length $s \in \mathbb{N}$, any degree of parallelism $k \in \mathbb{N}$ and slice length $\tau \in \mathbb{N}$, running SPS(\mathcal{J}, k, τ) indefinitely (i.e., $|\mathcal{J}| \rightarrow \infty$) requires memory*

$$\text{Peak}(k, \tau, s) \triangleq s \cdot k + \frac{1}{2} (\tau \cdot k + \tau + k - \gcd(\tau, k)).$$

Moreover, $\text{Peak}(k, \tau, s)$ is increasing in k when fixing τ and s .

LEMMA 2 (Feasible Parallelism of SPS). *Fix a job sequence \mathcal{J} with identical prompt length $s \in \mathbb{N}$ and a slice length $\tau \in \mathbb{N}$. Define the maximum memory-feasible degree of parallelism of STAGGERED-PIPELINESCHEDULE (SPS) as*

$$k^*(\tau, s) \triangleq \max \{k \in \mathbb{N} \mid \text{Peak}(k, \tau, s) \leq M\}. \quad (1)$$

where $\text{Peak}(k, \tau, s)$ is the peak memory usage of the schedule produced by SPS defined in Lemma 1. Then, the maximum memory-feasible degree of parallelism $k^*(\tau, s)$ can be lower bounded as

$$k^*(\tau, s) \geq \left\lfloor \frac{2M - \tau + 1}{2s + \tau + 1} \right\rfloor.$$

Proof of Lemma 1. Let the jobs be indexed $i = 0, 1, \dots$ according to the start time order assigned by SPS. Recall that the start time of job i is $t_i^{(\text{start})} = \lfloor i \cdot \tau/k \rfloor$, and each job runs for τ rounds.

Since $t_{i+k}^{(\text{start})} = \lfloor (i+k) \tau/k \rfloor = t_i^{(\text{start})} + \tau$, job i completes immediately before job $i+k$ starts. Therefore, the set of active jobs \mathcal{B}_t at any time $t = q\tau + \rho$ (with any integers $q \geq 1$ and $0 \leq \rho \leq \tau - 1$) always consists

of exactly k jobs. Each such job can be uniquely associated with a relative index $x \in \{0, \dots, k-1\}$ such that its start time is either $q\tau + \delta_x$ or $(q-1)\tau + \delta_x$, where $\delta_x \triangleq \lfloor x\tau/k \rfloor$ represents the start time offset within a period. Therefore, we can count the total memory usage, $S(t)$, at time t :

$$\begin{aligned} S(t) &= \sum_{i \in \mathcal{B}_t} (s + t - t_i^{(\text{start})} + 1) = k \cdot s + \sum_{x: \delta_x \leq \rho} (\rho - \delta_x + 1) + \sum_{x: \delta_x > \rho} (\tau + \rho - \delta_x + 1) \\ &= k \cdot s + k(\rho + 1) - \sum_{x=0}^{k-1} \delta_x + \sum_{x: \delta_x > \rho} \tau = k \cdot s + k(\rho + 1) - \sum_{x=0}^{k-1} \delta_x + (k - c(\rho))\tau, \\ &= k \cdot s + k\tau - \sum_{x=0}^{k-1} \delta_x + k(\rho + 1) - c(\rho)\tau \end{aligned}$$

where auxiliary notation $c(\rho) \triangleq |\{x \in \{0, \dots, k-1\} : \delta_x \leq \rho\}|$ is the number of jobs that start at or before offset ρ within a period. Note that $c(\rho) = \lceil k(\rho + 1)/\tau \rceil$, which implies $c(\rho) \cdot \tau \geq k(\rho + 1)$. Thus, the term $k(\rho + 1) - c(\rho)\tau$ is non-positive and the peak memory usage is bounded by:

$$\text{Peak}(k, \tau, s) = \max_{0 \leq \rho \leq \tau-1} S(t) \leq k \cdot s + k\tau - \sum_{x=0}^{k-1} \lfloor x\tau/k \rfloor.$$

The sum $\sum_{x=0}^{k-1} \lfloor x\tau/k \rfloor$ counts the number of positive integer points $(i, j) \in \mathbb{N}^2$ such that $0 < i < k$ and $0 < j \leq i \cdot \tau/k$. This corresponds to the number of integer points strictly inside the rectangle defined by $(0, 0)$ and (k, τ) that lie on or below the diagonal line connecting these two points. The number of integer points on the diagonal itself, excluding the endpoints, is $\gcd(k, \tau) - 1$ (where $\gcd(\cdot, \cdot)$ is the greatest common divisor). By symmetry, the number of points below the diagonal is half the number of off-diagonal points. Therefore, the sum is:

$$\sum_{x=0}^{k-1} \lfloor x\tau/k \rfloor = \frac{\overbrace{(k-1)(\tau-1)}^{\text{points in rectangle}} + \overbrace{(\gcd(k, \tau) - 1)}^{\text{points on diagonal}}}{2}.$$

Substituting this into the bound for $\text{Peak}(k, \tau, s)$:

$$\text{Peak}(k, \tau, s) \leq k \cdot s + k\tau - \frac{(k-1)(\tau-1) + \gcd(k, \tau) - 1}{2} = s \cdot k + \frac{k\tau + k + \tau - \gcd(k, \tau)}{2}.$$

and the equality is attained at every $t = q\tau - 1$ for $q \geq 1$.

To prove that $\text{Peak}(k, \tau, s)$ is monotone in k when fixing τ and s , we have

$$\text{Peak}(k+1, \tau, s) - \text{Peak}(k, \tau, s) = s + \frac{\tau + 1 - \gcd(k+1, \tau) + \gcd(k, \tau)}{2} \geq s + \frac{\tau + 1 - \tau + 1}{2} \geq s + 1,$$

which completes the proof of Lemma 1 as desired. \square

Proof of Lemma 2. By Lemma 1, the condition $\text{Peak}(k, \tau, s) \leq M$ is equivalent to

$$k(2s + \tau + 1) \leq 2M - \tau + \gcd(\tau, k).$$

By $\gcd(\tau, k) \geq 1$, we can choose

$$\left\lfloor \frac{2M - \tau + 1}{2s + \tau + 1} \right\rfloor \leq \frac{2M - \tau + \gcd(\tau, k)}{2s + \tau + 1}$$

as a valid lower bound for the maximum memory-feasible degree of parallelism $k^*(\tau, s)$. \square

We now proceed to prove Theorem 1. At the heart of our analysis is the notion of *memory-time area* (Definition 1), which quantifies the total KV-cache resources consumed by a job over its execution: it accounts for both the fixed prompt memory (s) and the linearly growing cache from o generated tokens. See the colored triangles (or more generally, trapezoids) in Figure 2, which illustrates this memory-time resource consumption. This geometric perspective yields a clean resource accounting principle: the total memory-time area consumed by any feasible schedule cannot exceed the area supplied by the memory budget M over time.

DEFINITION 1 (MEMORY-TIME AREA). For a job with prompt length s and response length o , its *memory-time area* is defined as

$$A(o, s) \triangleq s \cdot o + \frac{o(o+1)}{2}.$$

This quantity represents the total memory-time resources consumed by the job over its execution.

Our goal is to compare the packing efficiency of the optimal scheduler with that of SPS. Leveraging the geometric perspective above, Lemma 3 establishes a fundamental lower bound on the optimal flow time by observing that even the best schedule must allocate at least $A(\tau, s)$ area per job (for jobs with response length $\geq \tau$), and this area must be packed into a time horizon constrained by M . Conversely, Lemma 4 captures the *packing efficiency* of SPS: it shows that the average time per job in SPS is nearly proportional to the area-per-unit-memory, up to a small constant factor depending on the degree of parallelism. Together, these lemmas bridge memory usage and flow time, allowing us to compare SPS directly to the information-theoretic optimum via area-based reasoning.

LEMMA 3 (Area-Based Lower Bound on Optimal Flow Time). *Consider any instance with n jobs, each having prompt length s and response length at least τ . Then the optimal total flow time OPT satisfies*

$$\text{OPT} \geq \frac{n(n+1)}{2} \cdot \frac{A(\tau, s)}{M}.$$

LEMMA 4 (Area-Based Packing Efficiency of SPS). *For any integers $s \geq 0$ and $\tau \geq 1$, let $k^*(\tau, s)$ denote the maximum memory-feasible degree of parallelism defined in Lemma 2 (see Eqn. (1)). Then*

$$\frac{\tau}{k^*(\tau, s)} < \left(1 + \frac{2}{k^*(\tau, s)}\right) \cdot \frac{A(\tau, s)}{M}.$$

To gain more intuition behind these bounds, observe that the ratio $M/A(\tau, s)$ can be interpreted as an upper bound on the *throughput* (jobs per round) achievable by any feasible schedule—particularly the optimal clairvoyant scheduler. Meanwhile, $k^*(\tau, s)/\tau$ represents the effective throughput of SPS. In this sense, Lemma 3 lower bound the optimal total flow time via its throughput limit, while Lemma 4 shows that SPS achieves nearly optimal throughput, up to a small multiplicative factor in the parallelism dimension.

Below, we prove Lemmas 3 and 4. Using these results, we establish the asymptotic approximation ratio of $1 + o(1)$ stated in Theorem 1 for the large-memory regime. The proof of the (non-asymptotic) approximation ratio of 2 for general identical-job instances—also stated in Theorem 1—is deferred to Section EC.2.1.

Proof of Lemma 3. Let $C_1 \leq C_2 \leq \dots \leq C_n$ denote the completion times of the jobs in an optimal schedule. For each index $i \in [n]$, consider the first i jobs to complete (i.e., those with completion times C_1, \dots, C_i). Each of these i jobs has response length at least τ , and thus consumes memory-time area at least $A(\tau, s)$ (by Definition 1). Therefore, the total memory-time area consumed by these i jobs is at least $i \cdot A(\tau, s)$. On the other hand, during the first C_i rounds, the total memory available per round is at most M , so the total memory-time area supplied by the system up to time C_i is at most $M \cdot C_i$. Since the consumed area cannot exceed the supplied area, we have $i \cdot A(\tau, s) \leq M \cdot C_i$, which implies $C_i \geq \frac{i \cdot A(\tau, s)}{M}$. Summing over all $i \in [n]$ yields

$$\text{OPT} = \sum_{i=1}^n C_i \geq \sum_{i=1}^n \frac{i \cdot A(\tau, s)}{M} = \frac{n(n+1)}{2} \cdot \frac{A(\tau, s)}{M},$$

as claimed. □

Proof of Lemma 4. Define auxiliary notation $k \triangleq k^*(\tau, s)$. It suffices to show that

$$(k+2)\left(s + \frac{\tau+1}{2}\right) > M.$$

By definition of k (i.e., maximum memory-feasible degree of parallelism), we have $\text{Peak}(k+1, \tau, s) > M$. Applying Lemma 1,

$$\begin{aligned} M &< s(k+1) + \frac{\tau(k+1) + \tau + (k+1) - \gcd(k+1, \tau)}{2} \\ &\leq s(k+1) + \frac{\tau(k+1) + \tau + (k+1) - 1}{2} = sk + s + \frac{\tau k}{2} + \frac{k}{2} + \tau. \end{aligned}$$

Now observe that

$$(k+2)\left(s + \frac{\tau+1}{2}\right) = sk + s + \frac{\tau k}{2} + \frac{k}{2} + \tau + (s+1).$$

Since $s \geq 0$, the numerator exceeds the upper bound on M derived above. Hence,

$$(k+2)\left(s + \frac{\tau+1}{2}\right) > M,$$

which is equivalent to the desired inequality. □

Proof of approximation ratio $1 + o(1)$ in Theorem 1. Let $n = |\mathcal{J}|$. Under STAGGERED-PIPELINE-SCHEDULE (SPS) with parameters (k, τ) , the completion time of the i -th job (indexed from 0) is $\lfloor i\tau/k \rfloor + \tau$. Thus,

$$\text{FLOWTIME[SPS]} = \sum_{i=0}^{n-1} \left(\left\lfloor \frac{i\tau}{k} \right\rfloor + \tau \right) \leq n\tau + \frac{n(n-1)\tau}{2k}. \quad (2)$$

Combining this with the area-based lower bound from Lemma 3,

$$\text{OPT} \geq \frac{n(n+1)}{2} \cdot \frac{A(\tau, s)}{M},$$

we decompose the approximation ratio as

$$\frac{\text{FLOWTIME[SPS]}}{\text{OPT}} \leq \underbrace{\frac{n\tau}{\text{OPT}}}_{\text{(I)}} + \underbrace{\frac{\frac{n(n-1)\tau}{2k}}{\text{OPT}}}_{\text{(II)}}.$$

Bounding Term (I). Using the trivial lower bound $\text{OPT} \geq n\tau$, we have $\text{(I)} \leq 1$. Alternatively, applying Lemma 3 and then Lemma 4,

$$\text{(I)} \leq \frac{n\tau}{\frac{n(n+1)}{2} \cdot \frac{A(\tau, s)}{M}} = \frac{2\tau}{(n+1) \cdot \frac{A(\tau, s)}{M}} < \frac{2\tau}{(n+1) \cdot \frac{k}{\tau(1+2/k)}} = \frac{2k+4}{n+1}.$$

Hence,

$$\text{(I)} \leq \min\left\{1, \frac{2k+4}{n+1}\right\}.$$

Bounding Term (II). Again using Lemma 3 and Lemma 4,

$$\text{(II)} \leq \frac{\frac{n(n-1)\tau}{2k}}{\frac{n(n+1)}{2} \cdot \frac{A(\tau, s)}{M}} = \frac{n-1}{n+1} \cdot \frac{M\tau}{k \cdot A(\tau, s)} < \frac{n-1}{n+1} \cdot \left(1 + \frac{2}{k}\right).$$

Combining the Bounds. Summing the two terms yields

$$\frac{\text{FLOWTIME[SPS]}}{\text{OPT}} < \min\left\{1, \frac{2k+4}{n+1}\right\} + \frac{n-1}{n+1} \cdot \left(1 + \frac{2}{k}\right). \quad (3)$$

When the prompt length s and response length o are fixed, the dominant term in the right-hand side of (3) as $n \rightarrow \infty$ is term (II), which approaches $1 + 2/k$. More precisely, consider the regime where both the KV-cache memory budget $M \rightarrow \infty$ and the number of jobs $n \rightarrow \infty$ satisfy $M = o(n)$. Since $k = \Theta(M)$, we have $k \rightarrow \infty$ and $k/n \rightarrow 0$. Thus, term (I) is bounded by $O(k/n) = o(1)$, while term (II) approaches 1. Consequently, the overall approximation ratio converges to $1 + o(1)$, as desired. \square

REMARK 1. It can be verified that the right-hand side of (3) is at most $2 + \frac{1}{k}$. Thus, this also shows that the approximation ratio is at most 3 for general identical-job instances under memory-time area analysis framework. To tighten this bound to 2, we require a specialized analysis that exploits the structural properties of OPT for identical jobs. Its formal proof can be found in Section EC.2.1.

Algorithm 2: GEOMETRIC-SLICING-ALGORITHM (GSA)

Input: n jobs with known prompt length s and unknown response lengths $\{o_i\}_{i \in [n]}$,
 KV-cache memory budget M , scaling factor $\alpha > 1$

- 1 Let $\ell = \lfloor \log_\alpha (M - s) \rfloor, \beta = (M - s)/\alpha^\ell$; // ensures $1 \leq \beta < \alpha$ and $\beta \cdot \alpha^\ell = M - s$
- 2 Initialize geometric slice length $\hat{\tau} \leftarrow \beta$ and job set $\mathcal{T} \leftarrow [n]$;
- 3 **while** $\mathcal{T} \neq \emptyset$ **do**
- 4 Let $\tau \leftarrow \lfloor \hat{\tau} \rfloor$; // integer slice length used in this phase
- 5 Invoke STAGGERED-PIPELINE-SCHEDULE($\mathcal{T}, k^*(\tau, s), \tau$); // $k^*(\tau, s)$ defined in (1)
- 6 Update set $\mathcal{T} \leftarrow \{i \in \mathcal{T} \mid \text{job } i \text{ is not completed}\}$;
- 7 Update geometric slice length $\hat{\tau} \leftarrow \alpha \cdot \hat{\tau}$;

3.2. Algorithm Overview of GEOMETRIC-SLICING-ALGORITHM

In this section, we present the GEOMETRIC-SLICING-ALGORITHM. We start by giving an algorithm overview of it and then state its competitive ratio guarantee in Theorem 2. Its competitive ratio analysis is deferred to Sections 4 and 5.

Algorithm Overview. The GEOMETRIC-SLICING-ALGORITHM (GSA) is built on a simple yet powerful principle: *when job response lengths are unknown, the scheduler should iteratively guess their response length using a geometrically increasing time scale, and in each phase, execute a memory-efficient pipeline schedule based on the current guess.*

Specifically, given the set of unfinished jobs, GSA processes all of them in successive phases. Each phase $p = 0, 1, 2, \dots$ is defined by a *slice length* $\hat{\tau}_p$, which serves as the current hypothesis for job duration. The algorithm uses the integer slice length $\tau_p = \lfloor \hat{\tau}_p \rfloor$ when invoking STAGGERED-PIPELINE-SCHEDULE (SPS) defined in Procedure 1.

The algorithm is parameterized by a *scaling factor* $\alpha > 1$ (e.g., $\alpha = 2$ for doubling). The initial slice length $\hat{\tau}_0$ is set to the smallest value of the form $(M - s)/\alpha^\ell$ that is at least 1. This choice ensures that the geometric sequence $\hat{\tau}_p = \alpha^p \cdot \hat{\tau}_0$ will eventually reach the maximum feasible response length $M - s$, i.e., the largest response length that can be accommodated within the memory budget.¹¹

In each phase $p = 0, 1, 2, \dots$, GSA invokes SPS on the current job set \mathcal{T}_p , using:

- slice length $\tau = \tau_p$, and
- the maximum memory-feasible degree of parallelism $k^*(\tau_p, s)$, as defined in Lemma 2 (see Eq. (1)).

¹¹ This initialization is designed to optimize the theoretical analysis. Using $\hat{\tau}_0 = 1$ yields a slightly worse constant factor, and requires more discussions on the boundaries, e.g., when $\tau > M - s$. In practice (and in our numerical experiments (Section EC.1)), this initialization $\hat{\tau}_0 = \beta$ can be treated as a tunable parameter.

During this phase, every job in \mathcal{T}_p is scheduled by SPS and allowed to run for up to τ_p rounds. Jobs whose true response length satisfies $o_i \leq \tau_p$ complete successfully and are removed from the system. The remaining jobs (those with $o_i > \tau_p$) are killed at the end of the phase—their partial progress is discarded, and they will be restarted in the next phase. After the phase, the algorithm updates the job set to $\mathcal{T}_{p+1} \leftarrow \mathcal{T}_p \setminus \{\text{completed jobs}\}$ and scales the slice length geometrically:

$$\widehat{\tau}_{p+1} \leftarrow \alpha \cdot \widehat{\tau}_p,$$

This geometric growth guarantees that for any job i , there exists a phase p_i such that $\tau_{p_i} \geq o_i$, ensuring eventual completion.¹² See Algorithm 2 for a formal description of GEOMETRIC-SLICING-ALGORITHM.

Comparison with “let-long-jobs-finish” heuristics in prior work. Many non-clairvoyant schedulers—both in prior theoretical work (e.g., Chen et al., 2025) and in practice (e.g., First-Come-First-Served (FCFS) in Kwon et al., 2023)—adopt a “let-long-jobs-finish” heuristic: they avoid preempting running jobs unless the memory budget is exceeded, in an effort to minimize restarts and the associated wasted computation. While intuitive, this strategy can lead to significant efficiency loss by blocking memory for extended periods and limiting parallelism when considering the flow time objective.

In contrast, our proposed GSA employs a more aggressive *early-killing* strategy: it systematically terminates all unfinished jobs at the end of each geometric phase, regardless of their progress. The following example illustrates that this distinction plays a key role in enabling GSA to potentially outperform the aforementioned heuristics.

EXAMPLE 2 (LONG-JOB TRAP FOR CONSERVATIVE HEURISTICS). Fix a sufficiently large integer $\ell \in \mathbb{N}$. Consider an instance with $n \geq 2$ jobs, each having prompt length $s = 2^\ell$, and response length $o_i = 1 + (2^\ell - 1) \cdot \mathbb{1}\{i = 1\}$, under a KV-cache memory budget of $M = 2^{\ell+1}$. (Namely, the instance contains a single “long” job and $n - 1$ “short” jobs. The KV-cache memory budget is set such that at most one job can be active at any time.)

Consider a non-clairvoyant “let-long-jobs-finish” heuristic ALG that never kills the long job (i.e., job 1). We further assume that it sequentially processes all jobs in an order chosen uniformly at random, as jobs are not distinguishable before execution. Suppose the long job is the k -th job to finish ($1 \leq k \leq n$). Then the total flow time consists of three parts: (i) the first $k - 1$ short jobs contribute $\sum_{\ell=1}^{k-1} \ell$; (ii) the long job finishes at time $(k - 1) + 2^\ell$, contributing $k - 1 + 2^\ell$; and (iii) the remaining $n - k$ short jobs wait for the long job, each contributing its completion time $\ell + 2^\ell - 1$. Summing these gives a total flow time of

$$\frac{n(n+1)}{2} + (n - k + 1)(2^\ell - 1).$$

¹² The geometric increase of the slice length is essential for handling arbitrary unknown response lengths while maintaining a bounded number of restarts per job.

Since the execution order is uniform, k is uniformly distributed in $\{1, \dots, n\}$, so $\mathbb{E}[n - k + 1] = (n + 1)/2$. Thus, the expected flow time is

$$\text{FLOWTIME[ALG]} = \frac{n(n+1)}{2} + \frac{n+1}{2}(2^\ell - 1) = \frac{n+1}{2} \cdot (n + 2^\ell - 1).$$

In contrast, under GEOMETRIC-SLICING-ALGORITHM (GSA) with scaling factor $\alpha = 2$, in the first phase, it invokes STAGGERED-PIPELINE-SCHEDULE (SPS) with slice length $\tau = 1$ and degree of parallelism $k^*(\tau, s) = 1$ for all n jobs. All $n - 1$ short jobs are completed after this phase. In each phase $k \in [2 : \ell]$, it invokes SPS with slice length $\tau = 2^k$ and degree of parallelism $k^*(\tau, s) = 1$ for the long job, and this long job is completed in the ℓ -th phase. Thus, the total flow time of GSA satisfies

$$\text{FLOWTIME[GSA]} \leq \underbrace{\frac{1}{2} \cdot (n+2)(n-1)}_{\text{flow time from short jobs}} + \underbrace{n + 2 + 4 + \dots + 2^\ell - 1 + 2^\ell}_{\text{flow time from long job}} = \frac{(n+2)(n-1)}{2} + n + 2^{\ell+1} - 2,$$

where the inequality accounts for the worst executing order of n jobs in the first phase when invoking SPS.

Finally, the optimal clairvoyant schedule processes all $n - 1$ short jobs first and then processes the long job, with an optimal flow time of

$$\text{FLOWTIME[OPT]} = \frac{n(n+1)}{2} + 2^\ell - 1.$$

When both n and ℓ grow to infinity with $\ell = \Omega(n)$, the competitive ratios satisfy

$$\frac{\text{FLOWTIME[ALG]}}{\text{FLOWTIME[OPT]}} \rightarrow n \quad \text{and} \quad \frac{\text{FLOWTIME[GSA]}}{\text{FLOWTIME[OPT]}} \rightarrow 2. \quad \square$$

Competitive Ratio Guarantee. While the previous example illustrated that proactively killing and restarting the long job in GSA is sometimes indispensable, even though it might increase restart waste. We now turn to the first main theoretical result of this paper. Specifically, GSA achieves a *constant competitive ratio for all problem instances*. Theorem 2 first states its competitive ratio guarantee for an arbitrary scaling factor α , and then presents the optimized competitive ratios for general instances and large-memory instances obtained by tuning α optimally.

THEOREM 2 (Competitive Ratio Guarantee of GSA). *For any $\alpha \in (1, \infty)$, the competitive ratio of the non-clairvoyant scheduler GEOMETRIC-SLICING-ALGORITHM (GSA) with scaling factor α is at most*

$$\Gamma(\text{GSA}) \leq \left(2 + \frac{2}{\alpha-1}\right) \left(\alpha^2 \left(1 + \frac{2}{k_{\min}}\right) + \alpha + \frac{\alpha}{\alpha-1}\right)$$

where $k_{\min} \geq 1$ is the minimum degree of parallelism for the given input instance.

Moreover, by optimally tuning scaling factor $\alpha = (7 + \sqrt{13})/6 \approx 1.7676$, the competitive ratio guarantee satisfies

$$\Gamma(\text{GSA}) = \frac{92 + 26\sqrt{13}}{3} \approx 61.9148$$

and in the large memory regime (i.e., $k_{\min} \rightarrow \infty$),¹³ by setting scaling factor $\alpha = 2$, the competitive ratio guarantee converges to

$$\lim_{k_{\min} \rightarrow \infty} \Gamma(\text{GSA}) = 32.$$

The proof of Theorem 2 proceeds in two main steps. Since the optimal clairvoyant schedule may be complex and difficult to characterize directly, we first consider the clairvoyant setting and design a clairvoyant greedy algorithm. We then establish that this greedy algorithm achieves a constant-factor approximation to the optimal clairvoyant schedule (Theorem 3) in Section 4. In the second step (Section 5), we bound the competitive ratio between GSA and this clairvoyant greedy algorithm, thereby linking the performance of our non-clairvoyant algorithm to the offline optimum.

4. Constant-Approximation Algorithm in Clairvoyant Environment

In this section, we temporarily depart from our non-clairvoyant base model and consider the clairvoyant variant in which the scheduler knows all job response lengths in advance. We design a greedy algorithm—GEOMETRIC-BATCHING-ALGORITHM (GBA)—that batches jobs into batches based on their response lengths and then invokes our subroutine STAGGERED-PIPELINE-SCHEDULE (SPS). We show that this algorithm achieves a constant-factor approximation to the optimal clairvoyant schedule. Besides its own practical and theoretical interests, this result serves as a crucial intermediate step in establishing the competitive ratio guarantee of the non-clairvoyant GEOMETRIC-SLICING-ALGORITHM (GSA).

Algorithm Overview. GEOMETRIC-BATCHING-ALGORITHM (GBA) is the clairvoyant counterpart of GSA, designed for the setting where all response lengths $\{o_i\}$ are known. Like GSA, it proceeds in geometric phases with target slice length $\widehat{\tau}_p$ and integer slice length $\tau_p = \lfloor \widehat{\tau}_p \rfloor$ used by SPS. The algorithm initializes $\widehat{\tau}_0$ to $\beta = (M - s)/\alpha^\ell$ where $\ell = \lfloor \log_\alpha (M - s) \rfloor$, ensuring that $\widehat{\tau}_0 \in [1, \alpha)$, and the sequence eventually hits the memory-limited boundary $M - s$ exactly. In each phase p , GBA schedules only the subset $J_p = \{i \in \mathcal{J} : \widehat{\tau}_p/\alpha < o_i \leq \widehat{\tau}_p\}$ —those jobs guaranteed to finish within τ_p rounds. It invokes STAGGERED-PIPELINE-SCHEDULE on this subset with the memory-feasible degree of parallelism $k^*(\tau_p, s)$ (Eqn. (1)), ensuring no restarts. After completion, these jobs are removed, and $\widehat{\tau}$ is scaled by α . Because GBA avoids unnecessary preemptions and aligns structurally with GSA, it serves as a near-optimal clairvoyant benchmark, enabling a constant-factor competitive analysis for GSA against OPT. See Algorithm 3 for details.

4.1. Approximation Guarantee of GBA

In this section, we present the theoretical approximation guarantee of GBA.

¹³ This occurs when the prompt length s and all response lengths o_i are negligible compared to the KV-cache memory budget M , so that high parallelism is feasible throughout execution.

Algorithm 3: GEOMETRIC-BATCHING-ALGORITHM (GBA)

Input: n jobs with known prompt length s and known response lengths $\{o_i\}_{i \in [n]}$,
 KV-cache memory budget M , scaling factor $\alpha > 1$

- 1 Let $\ell = \lfloor \log_\alpha (M - s) \rfloor, \beta = (M - s)/\alpha^\ell$; // ensures $1 \leq \beta < \alpha$ and $\beta \cdot \alpha^\ell = M - s$
- 2 Initialize geometric slice length $\widehat{\tau} \leftarrow \beta$ and job set $\mathcal{T} \leftarrow [n]$;
- 3 **for** $p = 0$ **to** ℓ **do**
- 4 Construct set $\mathcal{J}_p \leftarrow \{i \in \mathcal{T} \mid \widehat{\tau}/\alpha < o_i \leq \widehat{\tau}\}$; // jobs completed in this phase
- 5 Let $\tau \leftarrow \lfloor \widehat{\tau} \rfloor$; // integer slice length used in this phase
- 6 Invoke STAGGERED-PIPELINE-SCHEDULE($\mathcal{J}_p, k^*(\tau, s), \tau$); // $k^*(\tau, s)$ defined in (1)
- 7 Update set $\mathcal{T} \leftarrow \mathcal{T} \setminus \mathcal{J}_p$;
- 8 Update geometric slice length $\widehat{\tau} \leftarrow \alpha \cdot \widehat{\tau}$;

THEOREM 3 (Approximation Guarantee of GBA). *For any $\alpha \in (1, \infty)$, the approximation ratio of the clairvoyant scheduler GEOMETRIC-BATCHING-ALGORITHM (GBA) with scaling factor α is at most*

$$\Gamma(\text{GBA}) \leq \alpha^2 \cdot \left(1 + \frac{2}{k_{\min}}\right) + \alpha + \frac{\alpha}{\alpha - 1}$$

where $k_{\min} \triangleq \min_p k_p \geq 1$ is the minimum degree of parallelism for the given input instance.

Moreover, by optimally tuning scaling factor $\alpha = 4/3 \approx 1.3333$, the approximation guarantee is at most

$$\Gamma(\text{GBA}) = \frac{32}{3} \approx 10.6667,$$

and in the large memory regime (i.e., $k_{\min} \rightarrow \infty$), by setting scaling factor $\alpha = 1.5$, the approximation guarantee converges to

$$\lim_{k_{\min} \rightarrow \infty} \Gamma(\text{GBA}) = 6.75.$$

4.2. Analysis of GBA: Key Steps and Technical Lemmas

Our analysis of GBA (proof of Theorem 3) proceeds through a sequence of carefully orchestrated steps that connect the structure of GBA to an information-theoretic lower bound on the optimal total flow time OPT . At a high level, we extend the memory-time area argument (Definition 1) from the single-class setting (i.e., identical-job instances) used in Theorem 1 (Section 3.1) to a multi-class setting, where jobs are partitioned into classes based on their response lengths o_i .

Specifically, consider a fixed job set \mathcal{J} with $|\mathcal{J}| = n$. For brevity, we let GBA denote the total flow time of running GBA on \mathcal{J} , and OPT denote the optimal total flow time for \mathcal{J} . In GBA, the jobs processed in phase p are referred to as *class p* jobs and denoted by J_p . Let:

- $n_p \triangleq |J_p|$ be the number of jobs in class $p \in \{0, 1, \dots, \ell\}$,
- $\tau_p \triangleq \lfloor \hat{\tau}_p \rfloor = \lfloor \beta \alpha^p \rfloor$ be the integer slice length used in phase p ,
- $k_p \triangleq k^*(\tau_p, s)$ be the degree of parallelism used for class p .

For convenience, we also introduce auxiliary notations

$$N_{>p} \triangleq \sum_{q>p} n_q, \quad N_{\geq p} \triangleq \sum_{q \geq p} n_q,$$

as the number of jobs in classes strictly greater than p , and in classes greater than or equal to p , respectively.

The key steps of the analysis are as follows:

Step 1: Area-Based Lower Bound on OPT (Lemma 5). We extend the memory-time area argument from Lemma 3 which lower bounds the optimal total flow time OPT to the multi-class setting. Specifically, we decompose the optimal total flow time OPT into two components: (i) the *within-class cost*, capturing the flow time due to jobs within the same class, and (ii) the *between-class cost*, accounting for the delay that smaller jobs impose on larger ones. This decomposition yields a phase-aware lower bound on OPT.

Since jobs in phase p have response length strictly greater than $\beta \alpha^{p-1}$, their memory-time area is at least

$$A_p \triangleq A(\beta \alpha^{p-1}, s),$$

where $A(\cdot, \cdot)$ is defined in Definition 1. This leads to the following lower bound on OPT.

LEMMA 5 (Area-Based Lower Bound for OPT). *The optimal total flow time OPT satisfies*

$$\text{OPT} \geq \text{WITHINCLASS} + \text{BETWEENCLASSES},$$

where

$$\text{WITHINCLASS} \triangleq \sum_p \frac{A_p}{M} \cdot \frac{n_p(n_p + 1)}{2}, \text{ and } \text{BETWEENCLASSES} \triangleq \sum_p \frac{A_p}{M} \cdot N_{>p} n_p.$$

Step 2: Per-Class Packing Efficiency of GBA (Lemma 6). We next extend the packing efficiency analysis from Lemma 4 to the multi-class setting. Specifically, we establish a lemma that characterizes the scheduling efficiency of GBA, which invokes SPS independently on each class of jobs. As in the identical-job case, this lemma relates the average time per job in class p —captured by the ratio τ_p/k_p —to the memory-time area of that class, up to a multiplicative factor that depends on the scaling parameter α and the minimum degree of parallelism $k_{\min} \geq 1$.

LEMMA 6 (Area-Based Packing Efficiency of GBA). *For each class p induced by GBA with scaling factor $\alpha \in (1, \infty)$,*

$$\frac{\tau_p}{k_p} \leq \alpha^2 \cdot \left(1 + \frac{2}{k_p}\right) \cdot \frac{A_p}{M},$$

Step 3: Upper Bound on GBA via Packing Efficiency (Lemma 7). In this step, we leverage the per-class packing efficiency established in Step 2—namely, the bound on $\{\tau_p/k_p\}_p$ —to derive an upper bound on the total flow time of GBA. Specifically, this upper bound mirrors the decomposition used in the lower bound for OPT: it is obtained by summing over classes, and for each class p , it accounts for (i) the internal completion times of its jobs (via SPS), and (ii) the waiting time incurred due to all earlier classes. This parallel structure enables a direct comparison between GBA and OPT in the final analysis. To formalize this, we introduce two key quantities that capture the two components of the flow time. For each class p , define the *ladder term*

$$Q_p \triangleq n_p \cdot \tau_p + \sum_{i=0}^{n_p-1} \left\lfloor \frac{i \cdot \tau_p}{k_p} \right\rfloor, \quad (4)$$

which upper bounds the total completion time of the jobs in class p when scheduled in isolation via SPS, and the *class-prefix term*

$$S_p \triangleq \sum_{q < p} \left(\left\lfloor \frac{n_q \cdot \tau_q}{k_q} \right\rfloor + \tau_q \right), \quad (5)$$

which upper bounds the total waiting time experienced by jobs in class p due to execution of all earlier classes. With these definitions, the total flow time of GBA is bounded as follows.

LEMMA 7 (GBA Upper Bound via Packing Efficiency). *The total flow time of GBA satisfies*

$$\text{GBA} \leq \overline{\text{GBA}} \triangleq \sum_p (n_p \cdot S_p + Q_p).$$

where Q_p and S_p are defined in Eqn. (4) and Eqn. (5), respectively.

Step 4: Combining Bounds and Optimizing the Scaling Factor α . By combining the upper bound on GBA with the lower bound on OPT—using the memory-time area framework developed above—and leveraging the geometric progression of slice lengths, we obtain the approximation guarantee stated in Theorem 3. Optimizing the scaling factor α yields the constants given in Theorem 3: approximately 10.67 in the general case and 6.75 in the large-memory regime.

This structured approach not only establishes a constant-factor approximation guarantee for GBA, but also provides the analytical foundation for the competitive analysis of the non-clairvoyant GSA in Section 5.

4.3. Proofs in the Analysis of GBA

In this section, we include all the proofs of the technical lemmas and then establish Theorem 3.

LEMMA 5 (Area-Based Lower Bound for OPT). *The optimal total flow time OPT satisfies*

$$\text{OPT} \geq \text{WITHINCLASS} + \text{BETWEENCLASSES},$$

where

$$\text{WITHINCLASS} \triangleq \sum_p \frac{A_p}{M} \cdot \frac{n_p(n_p + 1)}{2}, \text{ and } \text{BETWEENCLASSES} \triangleq \sum_p \frac{A_p}{M} \cdot N_{>p} n_p.$$

Proof of Lemma 5. Following the argument in Lemma 3, let $C_1 \leq C_2 \leq \dots \leq C_n$ denote the completion times of the n jobs in an optimal schedule. By the memory-time area accounting principle, the total area consumed by the first i jobs is at least $\sum_{j=1}^i A(o_j, s)$, and this cannot exceed $M \cdot C_i$. Hence,

$$C_i \geq \frac{1}{M} \sum_{j=1}^i A(o_j, s).$$

Summing over all i , we obtain

$$\text{OPT} = \sum_{i=1}^n C_i \geq \frac{1}{M} \sum_{i=1}^n \sum_{j=1}^i A(o_j, s) = \frac{1}{M} \sum_{j=1}^n (n-j+1) \cdot A(o_j, s).$$

Since each job j belongs to some class p_j , and by construction $o_j > \beta \alpha^{p_j-1}$, we have $A(o_j, s) \geq A_{p_j}$. Therefore,

$$\text{OPT} \geq \frac{1}{M} \sum_{j=1}^n (n-j+1) \cdot A_{p_j}.$$

To minimize the right-hand side, the jobs should be ordered in non-decreasing order of A_{p_j} . Because A_p is strictly increasing in p , this is achieved by processing all jobs in class 0 first, then class 1, and so on up to class ℓ . Under this ordering, the jobs in class p occupy positions $j = N_{>p} + 1$ through $j = N_{\geq p}$, and for each such job, the coefficient $(n-j+1)$ equals $N_{>p} + i$, where $i \in \{1, \dots, n_p\}$ indexes the job within its class. Thus,

$$\begin{aligned} \text{OPT} &\geq \sum_p \sum_{i=1}^{n_p} (N_{>p} + i) \cdot \frac{A_p}{M} = \sum_p \left(N_{>p} n_p \cdot \frac{A_p}{M} + \frac{A_p}{M} \cdot \frac{n_p(n_p+1)}{2} \right) \\ &= \text{BETWEENCLASSES} + \text{WITHINCLASS}, \end{aligned}$$

which completes the proof. \square

LEMMA 6 (Area-Based Packing Efficiency of GBA). *For each class p induced by GBA with scaling factor $\alpha \in (1, \infty)$,*

$$\frac{\tau_p}{k_p} \leq \alpha^2 \cdot \left(1 + \frac{2}{k_p} \right) \cdot \frac{A_p}{M},$$

Proof of Lemma 6. By the maximality of k_p (see Lemma 2), we have

$$M < s(k_p + 1) + \frac{\tau_p(k_p + 1) + \tau_p + (k_p + 1) - 1}{2} \leq sk_p + s + \frac{\tau_p k_p}{2} + \tau_p + \frac{k_p}{2}.$$

Dividing both sides by A_p and multiplying by τ_p/k_p yields

$$\frac{\tau_p}{k_p} \cdot \frac{M}{A_p} < \frac{\tau_p s \left(1 + \frac{1}{k_p} \right) + \frac{\tau_p^2}{2} \left(1 + \frac{2}{k_p} \right) + \frac{\tau_p}{2}}{A_p}.$$

Let $y \triangleq \beta\alpha^{p-1}$, so that $A_p = A(y, s) = sy + \frac{y(y+1)}{2}$. Since $\tau_p \leq \alpha y$, substituting this upper bound and dividing numerator and denominator by y gives

$$\frac{\tau_p}{k_p} \cdot \frac{M}{A_p} \leq f_{k_p}(y),$$

where for any $k \geq 1$ and $y > 0$,

$$f_k(y) \triangleq \frac{\alpha s \left(1 + \frac{1}{k}\right) + \alpha^2 y \left(\frac{1}{2} + \frac{1}{k}\right) + \frac{\alpha}{2}}{s + \frac{y+1}{2}}.$$

By computing its derivative, it can be verified that $f_k(y)$ is non-decreasing in y . Recall that the initialization ensures $\beta\alpha^\ell = M - s$. Therefore, for any $p \leq \ell$,

$$y = \beta\alpha^{p-1} \leq \frac{M - s}{\alpha} \triangleq y_0.$$

Since f_{k_p} is non-decreasing, $f_{k_p}(y) \leq f_{k_p}(y_0)$. Substituting and simplifying, we obtain

$$f_{k_p}(y_0) = \frac{\alpha \left(\frac{s}{2} + M \left(\frac{1}{2} + \frac{1}{k_p}\right) + \frac{1}{2}\right)}{s + \frac{M-s}{2\alpha} + \frac{1}{2}}.$$

Dividing numerator and denominator by M and letting $\rho \triangleq s/M$, this becomes

$$f_{k_p}(y_0) = \frac{\alpha}{k_p} \cdot \frac{(k_p + 2) + k_p \rho + \frac{k_p}{M}}{2\rho + \frac{1 - \rho}{\alpha} + \frac{1}{M}} \triangleq \Psi(\alpha, \rho, k_p, M)$$

Finally, by computing its derivative, it can be verified that auxiliary function $\Psi(\alpha, \rho, k_p, M)$ is (i) strictly decreasing in ρ , and (ii) strictly increasing in M . Therefore, for any $\rho \geq 0$ and $M \geq 1$, we have

$$\Psi(\alpha, \rho, k_p, M) \leq \Psi(\alpha, 0, k_p, \infty) = \alpha^2 \cdot \left(1 + \frac{2}{k_p}\right).$$

Substituting this bound into the previous inequality gives

$$\frac{\tau_p}{k_p} \leq \alpha^2 \cdot \left(1 + \frac{2}{k_p}\right) \cdot \frac{A_p}{M},$$

which completes the proof. \square

LEMMA 7 (GBA Upper Bound via Packing Efficiency). *The total flow time of GBA satisfies*

$$\text{GBA} \leq \overline{\text{GBA}} \triangleq \sum_p (n_p \cdot S_p + Q_p).$$

where Q_p and S_p are defined in Eqn. (4) and Eqn. (5), respectively.

Proof of Lemma 7. By construction, GBA processes classes sequentially in increasing order of p . All jobs in class p begin execution only after all jobs in classes $q < p$ have completed. For any job in class p , its completion time equals:

$$\underbrace{(\text{total time spent on all prior classes})}_{\leq S_p} + \underbrace{(\text{its completion time within class } p \text{ under SPS})}_{\leq \tau_p + \left\lfloor \frac{i \cdot \tau_p}{k_p} \right\rfloor},$$

where $i \in \{0, \dots, n_p - 1\}$ indexes the job within the class. Summing over all n_p jobs in class p , the total contribution to flow time is at most $n_p \cdot S_p + Q_p$. Summing over all classes p yields the desired bound:

$$\text{GBA} \leq \sum_p (n_p \cdot S_p + Q_p)$$

which completes the proof as desired. \square

We are now ready to prove Theorem 3.

Proof of Theorem 3. We bound the total flow time of GBA by analyzing its decomposition into within-class and between-class components. Recall from Lemma 7 that

$$\text{GBA} \leq \overline{\text{GBA}} = \sum_p (n_p \cdot S_p + Q_p).$$

We bound the two terms separately.

Within-class ladder term. From the definition in Eqn. (4),

$$Q_p = n_p \tau_p + \sum_{i=0}^{n_p-1} \left\lfloor \frac{i \tau_p}{k_p} \right\rfloor \leq n_p \tau_p + \frac{\tau_p}{k_p} \cdot \frac{n_p(n_p - 1)}{2}.$$

By Lemma 6, we obtain

$$\sum_p Q_p \leq \sum_p n_p \tau_p + \sum_p \alpha^2 \cdot \left(1 + \frac{2}{k_p}\right) \cdot \frac{A_p}{M} \cdot \frac{n_p(n_p - 1)}{2}.$$

Noting that $\frac{n(n-1)}{2} < \frac{n(n+1)}{2}$ and $k_{\min} = \min_p k_p$ (as defined in the theorem), we obtain

$$\sum_p Q_p \leq \sum_p n_p \tau_p + \alpha^2 \cdot \left(1 + \frac{2}{k_{\min}}\right) \cdot \text{WITHINCLASS}.$$

Since each job i has response length o_i and $\tau_p \leq \alpha o_i$ for all $i \in J_p$, we have

$$\sum_p n_p \tau_p \leq \alpha \sum_{i=1}^n o_i \leq \alpha \cdot \text{OPT},$$

because the optimal schedule must spend at least o_i rounds on each job. Hence,

$$\sum_p Q_p \leq \alpha^2 \cdot \left(1 + \frac{2}{k_{\min}}\right) \cdot \text{WITHINCLASS} + \alpha \cdot \text{OPT}.$$

Between-class prefix term. By definition in Eqn. (5) and summation exchange,

$$\sum_p n_p S_p = \sum_q N_{>q} \left(\tau_q + \left\lfloor \frac{n_q \tau_q}{k_q} \right\rfloor \right) \leq (\text{I}) + (\text{II}),$$

where

$$(\text{I}) = \sum_q N_{>q} \tau_q, \quad (\text{II}) = \sum_q N_{>q} \cdot \frac{n_q \tau_q}{k_q}.$$

To bound (I), recall that $\hat{\tau}_p = \beta \alpha^p$ and $\tau_p = \lfloor \hat{\tau}_p \rfloor$. Then for any p ,

$$\sum_{q < p} \tau_q \leq \sum_{q < p} \hat{\tau}_q = \frac{\hat{\tau}_p - \beta}{\alpha - 1} \leq \frac{\tau_p + 1 - 1}{\alpha - 1} = \frac{\tau_p}{\alpha - 1}, \quad (6)$$

since $\beta \geq 1$ and $\tau_p \geq \hat{\tau}_p - 1$. Therefore,

$$(\text{I}) = \sum_p n_p \sum_{q < p} \tau_q \leq \frac{1}{\alpha - 1} \sum_p n_p \tau_p \leq \frac{\alpha}{\alpha - 1} \cdot \text{OPT}.$$

For (II), applying Lemma 6 gives

$$(\text{II}) \leq \sum_q \alpha^2 \cdot \left(1 + \frac{2}{k_p} \right) \cdot N_{>q} \cdot \frac{A_q}{M} \cdot n_q \leq \alpha^2 \cdot \left(1 + \frac{2}{k_{\min}} \right) \cdot \text{BETWEENCLASSES}.$$

Thus,

$$\sum_p n_p S_p \leq \alpha^2 \cdot \left(1 + \frac{2}{k_{\min}} \right) \cdot \text{BETWEENCLASSES} + \frac{\alpha}{\alpha - 1} \cdot \text{OPT}.$$

Combining the bounds. Combining all the pieces above and using $\text{OPT} \geq \text{WITHINCLASS} + \text{BETWEENCLASSES}$ from Lemma 5, we obtain

$$\begin{aligned} \text{GBA} &\leq \overline{\text{GBA}} \leq \alpha^2 \cdot \left(1 + \frac{2}{k_{\min}} \right) \cdot (\text{WITHINCLASS} + \text{BETWEENCLASSES}) + \left(\alpha + \frac{\alpha}{\alpha - 1} \right) \cdot \text{OPT} \\ &\leq \left(\alpha^2 \cdot \left(1 + \frac{2}{k_{\min}} \right) + \alpha + \frac{\alpha}{\alpha - 1} \right) \cdot \text{OPT}. \end{aligned}$$

as claimed. To obtain the numerical constants, we optimize over $\alpha > 1$:

- In the worst case ($k_{\min} = 1$), the bound becomes $3\alpha^2 + \alpha + \frac{\alpha}{\alpha - 1}$. Minimizing this expression yields $\alpha = 4/3$ and a value of $32/3 \approx 10.6667$.
- In the large-memory regime ($k_{\min} \rightarrow \infty$), the bound reduces to $\alpha^2 + \alpha + \frac{\alpha}{\alpha - 1}$. Minimization gives $\alpha = 3/2$ and a value of 6.75.

This completes the proof of Theorem 3. \square

5. Competitive Ratio Analysis of Geometric Slicing Algorithm

In this section, we continue to analyze the performance of GEOMETRIC-SLICING-ALGORITHM (GSA) introduced in Section 3.

The analysis of GSA proceeds by leveraging the structural similarity between the non-clairvoyant GSA and its clairvoyant counterpart GBA (analyzed in Section 4). The core insight is that, despite operating without knowledge of job response lengths, GSA’s geometric phase design ensures that its extra cost—due to processing all remaining jobs in every phase—can be bounded by a constant factor times the cost of GBA. This yields a two-step competitive analysis: first bounding GSA against GBA, then combining with GBA’s approximation guarantee against OPT.

5.1. Key Steps and Technical Lemmas

To analyze the flow time of GSA, we adopt a decomposition analogous to that used for GBA in Section 4.2. The key distinction lies in how jobs are scheduled across phases: whereas GBA processes only class- p jobs in phase p , GSA—operating without knowledge of response lengths—processes *all remaining jobs* in every phase. This non-clairvoyant behavior inflates the flow time, which we decompose into three components: (i) the *ladder term* Q_p , identical to that in GBA (see Eqn. (4)), capturing internal completion times within a class; (ii) the *spillover term* Δ_p , reflecting the extra runtime incurred by jobs that span multiple phases; and (iii) the *phase-prefix term* T_p , representing waiting time due to all prior phases, now amplified by the larger active batches in GSA.

We reuse the notation from the GBA analysis (see Section 4.2): J_p and n_p denote the set and number of jobs in class p ; $\tau_p = \lfloor \hat{\tau}_p \rfloor = \lfloor \beta \alpha^p \rfloor$ is the integer slice length used by SPS in phase p ; k_p is the corresponding degree of parallelism; and $N_{>p}$, $N_{\geq p}$ are the numbers of jobs in classes strictly greater than p , and in classes greater than or equal to p , respectively. The key steps are as follows:

Step 1: Upper Bound on GSA via Packing Efficiency (Lemma 8). For GSA, every unfinished job participates in all phases up to its completion. To capture this, we define two additional quantities for each phase p : the *phase spillover cost*

$$\Delta_p \triangleq \left\lceil \frac{N_{>p} \cdot \tau_p}{k_p} \right\rceil, \quad (7)$$

which upper bounds the extra rounds needed to accommodate jobs from later classes, and the *phase-prefix cost*

$$T_p \triangleq \sum_{q < p} \left(\left\lfloor \frac{N_{\geq q} \cdot \tau_q}{k_q} \right\rfloor + \tau_q \right), \quad (8)$$

which accounts for the cumulative time spent on all prior phases. With these definitions, the total flow time of GSA is bounded as follows.

LEMMA 8 (GSA Upper Bound via Packing Efficiency). *The total flow time of GSA satisfies*

$$\text{GSA} \leq \sum_p n_p (T_p + \Delta_p) + \sum_p Q_p,$$

where Q_p , Δ_p , and T_p are as defined in Eqn. (4), Eqn. (7), and Eqn. (8), respectively.

Step 2: Upper Bound on Spillover Cost (Lemma 9). We show that the total spillover cost incurred by GSA is bounded by the prefix cost of its clairvoyant counterpart GBA plus one ladder term. Specifically, we establish the following bound.

LEMMA 9 (Upper Bound on Spillover Cost of GSA). *The total spillover cost of GSA satisfies*

$$\sum_p n_p \cdot \Delta_p \leq \sum_p n_p \cdot S_p + \sum_p Q_p.$$

We emphasize that this inequality holds only in aggregate over all phases; it may be violated for individual phases (i.e., $n_p \cdot \Delta_p \leq n_p \cdot S_p + Q_p$ need not hold for a fixed p).

Step 3: Upper Bound on Inflated Prefix Cost (Lemma 10). We bound the inflated phase-prefix term T_p using a novel counting inequality (see Lemma 11) that relates the ceiling of aggregate job counts to the sum of individual contributions. Combined with the geometric increment of slice lengths, this yields a bound on the total phase-prefix cost of GSA in terms of GBA's ladder and prefix terms.

LEMMA 10 (Upper Bound on Phase-Prefix Cost of GSA). *For any scaling factor $\alpha \in (1, \infty)$, the total phase-prefix cost of GSA satisfies*

$$\sum_p n_p \cdot T_p \leq \left(1 + \frac{2}{\alpha - 1}\right) \sum_p n_p \cdot S_p + \frac{2}{\alpha - 1} \sum_p Q_p.$$

Step 4: Combining Bounds and Optimizing the Scaling Factor α . By combining the upper bound on GSA (from Lemma 8) with the upper bound on GBA (i.e., $\overline{\text{GBA}}$ in Lemma 7) and the approximation guarantee of $\overline{\text{GBA}}$ relative to OPT established in Theorem 3,¹⁴ we obtain the competitive ratio stated in Theorem 2. Optimizing the scaling factor α yields the constants given in Theorem 2: approximately 61.92 in the general case and 32 in the large-memory regime.

This approach not only establishes the first constant-competitive algorithm for non-clairvoyant KV-cache scheduling but also demonstrates the power of geometric phase alignment in bridging clairvoyant and non-clairvoyant settings.

¹⁴ The analysis in Theorem 3 applies verbatim to $\overline{\text{GBA}}$. Though $\overline{\text{GBA}}$ is an upper bound on GBA and the proof compares this quantity directly to OPT.

5.2. Proofs in the Analysis of GSA

In this section, we include all the proofs of the technical lemmas and then establish Theorem 3.

LEMMA 8 (GSA Upper Bound via Packing Efficiency). *The total flow time of GSA satisfies*

$$\text{GSA} \leq \sum_p n_p (T_p + \Delta_p) + \sum_p Q_p,$$

where Q_p , Δ_p , and T_p are as defined in Eqn. (4), Eqn. (7), and Eqn. (8), respectively.

Proof. By construction, GSA processes all remaining jobs in every phase. Consider any job i that belongs to class p (i.e., it completes in phase p). Its contribution to the total flow time consists of three parts:

Time spent in prior phases: In each phase $q < p$, job i is active and contributes to the execution of the batch. The total time spent across all prior phases is exactly the duration of those phases, which is upper bounded by T_p as defined in Eqn. (8).

Spillover time in phase p : At the start of phase p , the active batch includes all unfinished jobs, namely the $N_{\geq p} = n_p + N_{>p}$ jobs from class p and later classes. The extra load from the $N_{>p}$ jobs from later classes increases the runtime of the phase. The additional rounds needed due to this “spillover” are upper bounded by $\Delta_p = \lceil N_{>p} \cdot \tau_p / k_p \rceil$, as in Eqn. (7).

Internal completion time within class p : Once the spillover effect is accounted for, the relative ordering of the n_p jobs in class p under SPS yields a total internal completion time bounded by the ladder term Q_p defined in Eqn. (4).

Summing over all jobs in class p , the total contribution to flow time is at most

$$n_p \cdot (T_p + \Delta_p) + Q_p.$$

Finally, summing over all phases p gives the desired upper bound:

$$\text{GSA} \leq \sum_p n_p (T_p + \Delta_p) + \sum_p Q_p,$$

which completes the proof. □

LEMMA 9 (Upper Bound on Spillover Cost of GSA). *The total spillover cost of GSA satisfies*

$$\sum_p n_p \cdot \Delta_p \leq \sum_p n_p \cdot S_p + \sum_p Q_p.$$

Proof of Lemma 9. Let $\gamma_p \triangleq \tau_p / k_p$. Since $\lceil x \rceil \leq x + 1$, we have

$$\Delta_p = \lceil N_{>p} \cdot \gamma_p \rceil \leq N_{>p} \cdot \gamma_p + 1.$$

Therefore,

$$\sum_p n_p \cdot \Delta_p \leq \sum_p N_{>p} n_p \cdot \gamma_p + \sum_p n_p.$$

Since $\tau_p \geq 1$ and $x < \lfloor x \rfloor + 1$, we obtain

$$n_p \cdot \gamma_p \leq \left\lfloor \frac{n_p \cdot \tau_p}{k_p} \right\rfloor + \tau_p.$$

Multiplying by $N_{>p}$ and summing gives

$$\sum_p N_{>p} n_p \cdot \gamma_p \leq \sum_p N_{>p} \left(\left\lfloor \frac{n_p \cdot \tau_p}{k_p} \right\rfloor + \tau_p \right) = \sum_p n_p \cdot S_p,$$

where the equality follows by swapping the order of summation in the definition of S_p (Eqn. (5)). Finally, by definition of Q_p in Eqn. (4), we have

$$\sum_p n_p \leq \sum_p n_p \cdot \tau_p \leq \sum_p Q_p,$$

Combining the bounds completes the proof. \square

LEMMA 10 (Upper Bound on Phase-Prefix Cost of GSA). *For any scaling factor $\alpha \in (1, \infty)$, the total phase-prefix cost of GSA satisfies*

$$\sum_p n_p \cdot T_p \leq \left(1 + \frac{2}{\alpha - 1}\right) \sum_p n_p \cdot S_p + \frac{2}{\alpha - 1} \sum_p Q_p.$$

The proof of Lemma 10 relies on the following technical claim.

LEMMA 11. *For any integers $n \geq 1$ and $k \geq 1$, the following inequality holds:*

$$n \cdot \left\lceil \frac{n}{k} \right\rceil \leq 2 \sum_{u=1}^n \left\lceil \frac{u}{k} \right\rceil.$$

Proof. Let $q \triangleq \lfloor n/k \rfloor$ and write $n = qk + r$, where $0 \leq r < k$. Then $\lceil n/k \rceil = q$ if $r = 0$, and $q + 1$ otherwise.

We first compute the sum on the right-hand side:

$$\sum_{u=1}^n \left\lceil \frac{u}{k} \right\rceil = \sum_{\ell=1}^q \ell \cdot k + (q+1) \cdot r = \frac{q(q+1)}{2} \cdot k + (q+1) \cdot r.$$

We now verify the inequality in both cases.

Case 1: $r = 0$. In this case, $n = qk$ and $\lceil n/k \rceil = q$. The left-hand side becomes $qk \cdot q = q^2k$, while the right-hand side is

$$2 \cdot \frac{q(q+1)}{2} \cdot k = q(q+1)k.$$

Since $q^2 \leq q(q+1)$, the inequality holds.

Case 2: $r > 0$. In this case, $\lceil n/k \rceil = q + 1$, and the left-hand side is

$$n \cdot (q + 1) = (qk + r)(q + 1).$$

The right-hand side is

$$2 \left(\frac{q(q+1)}{2} \cdot k + (q+1) \cdot r \right) = (q+1)(qk + 2r).$$

Thus, the desired inequality reduces to

$$qk + r \leq qk + 2r,$$

which holds since $r \geq 1$. This completes the proof as desired. \square

Proof of Lemma 10. We begin by expanding the left-hand side and decomposing $N_{\geq q} = n_q + N_{>q}$:

$$\sum_p n_p \cdot T_p = \sum_q N_{>q} \left(\tau_q + \left\lfloor \frac{N_{\geq q} \cdot \tau_q}{k_q} \right\rfloor \right).$$

Splitting the floor term and using $\lfloor a + b \rfloor \leq \lfloor a \rfloor + \lceil b \rceil$, we obtain

$$\sum_p n_p \cdot T_p \leq \underbrace{\sum_q N_{>q} \left(\tau_q + \left\lfloor \frac{n_q \cdot \tau_q}{k_q} \right\rfloor \right)}_{(I) \equiv \sum_p n_p \cdot S_p} + \underbrace{\sum_q N_{>q} \cdot \left\lceil \frac{N_{>q} \cdot \tau_q}{k_q} \right\rceil}_{(II)}.$$

We now bound term (II). Since τ_q is an integer,

$$(II) \leq \sum_q N_{>q} \cdot \tau_q \cdot \left\lceil \frac{N_{>q}}{k_q} \right\rceil.$$

Applying the counting inequality from 11, we have

$$N_{>q} \cdot \left\lceil \frac{N_{>q}}{k_q} \right\rceil \leq 2 \sum_{u=1}^{N_{>q}} \left\lceil \frac{u}{k_q} \right\rceil,$$

and thus

$$(II) \leq 2 \sum_q \tau_q \sum_{u=1}^{N_{>q}} \left\lceil \frac{u}{k_q} \right\rceil. \quad (9)$$

We now enumerate the $N_{>q}$ jobs in classes strictly above q by their class $t > q$ and within-class rank $r \in \{1, \dots, n_t\}$. By the definition of k and the monotonicity of **Peak** (Lemma 1), for $t > q$, we have $k_q \geq k_t$, which implies $1/k_q \leq 1/k_t$. Using this monotonicity,

$$\begin{aligned} \sum_{u=1}^{N_{>q}} \left\lceil \frac{u}{k_q} \right\rceil &\leq \sum_{t>q: n_t \geq 1} \sum_{r=1}^{n_t} \left(\left\lceil \frac{r}{k_t} \right\rceil + \sum_{v=q+1}^{t-1} \left\lceil \frac{n_v}{k_q} \right\rceil \right) \\ &\leq \sum_{t>q: n_t \geq 1} \sum_{r=1}^{n_t} \left(\left\lceil \frac{r}{k_t} \right\rceil + \sum_{v=q+1}^{t-1} \left\lceil \frac{n_v}{k_v} \right\rceil \right) \end{aligned}$$

Substituting into (9) and splitting the sum yields

$$(II) \leq 2 \cdot ((II.A) + (II.B)),$$

where

$$(II.A) \triangleq \sum_q \tau_q \sum_{t>q} \sum_{r=1}^{n_t} \left\lceil \frac{r}{k_t} \right\rceil, \text{ and } (II.B) \triangleq \sum_q \tau_q \sum_{t>q} n_t \sum_{v=q+1}^{t-1} \left\lceil \frac{n_v}{k_v} \right\rceil.$$

We now bound each term using the geometric increment of slice lengths. By Eqn. (6),

$$\sum_{q< t} \tau_q \leq \frac{\tau_t}{\alpha - 1}.$$

For (II.A), interchanging the order of summation gives

$$(II.A) = \sum_t \left(\sum_{q< t} \tau_q \right) \sum_{r=1}^{n_t} \left\lceil \frac{r}{k_t} \right\rceil \leq \frac{1}{\alpha - 1} \sum_t \tau_t \sum_{r=1}^{n_t} \left\lceil \frac{r}{k_t} \right\rceil.$$

Since τ_t is integral, we have

$$\tau_t \sum_{r=1}^{n_t} \left\lceil \frac{r}{k_t} \right\rceil = n_t \tau_t + \sum_{r=0}^{n_t-1} \tau_t \left\lceil \frac{r}{k_t} \right\rceil \leq Q_t,$$

where the inequality follows from $\tau_t \lfloor r/k_t \rfloor \leq \lfloor r\tau_t/k_t \rfloor$. Hence,

$$(II.A) \leq \frac{1}{\alpha - 1} \sum_t Q_t.$$

For (II.B), swapping summations yields

$$\begin{aligned} (II.B) &= \sum_t \left(\sum_{q< t} \tau_q \right) N_{>t} \left\lceil \frac{n_t}{k_t} \right\rceil \leq \frac{1}{\alpha - 1} \sum_t N_{>t} \tau_t \left\lceil \frac{n_t}{k_t} \right\rceil \\ &\leq \frac{1}{\alpha - 1} \sum_t N_{>t} \left(\left\lfloor \frac{n_t \tau_t}{k_t} \right\rfloor + \tau_t \right) = \frac{1}{\alpha - 1} \sum_p n_p \sum_{q< p} \left(\left\lfloor \frac{n_q \tau_q}{k_q} \right\rfloor + \tau_q \right) = \frac{1}{\alpha - 1} \sum_p n_p \cdot S_p. \end{aligned}$$

Combining the bounds on (I), (II.A), and (II.B), we obtain

$$\sum_p n_p \cdot T_p \leq \left(1 + \frac{2}{\alpha - 1} \right) \sum_p n_p \cdot S_p + \frac{2}{\alpha - 1} \sum_p Q_p,$$

which completes the proof of Lemma 10 as desired. \square

We are now ready to combine all technical pieces and establish Theorem 2 for GSA.

Proof of Theorem 2. Invoking Lemmas 8 to 10, we obtain

$$\begin{aligned} \text{GSA} &\leq \sum_p n_p (T_p + \Delta_p) + \sum_p Q_p \\ &\leq \sum_p n_p \cdot S_p + 2 \sum_p Q_p + \left(1 + \frac{2}{\alpha - 1} \right) \sum_p n_p \cdot S_p + \frac{2}{\alpha - 1} \sum_p Q_p \leq \left(2 + \frac{2}{\alpha - 1} \right) \overline{\text{GBA}} \end{aligned}$$

Invoking Theorem 3, we obtain¹⁴

$$\text{GSA} \leq \left(2 + \frac{2}{\alpha - 1} \right) \left(\alpha^2 \cdot \left(1 + \frac{2}{k_{\min}} \right) + \alpha + \frac{\alpha}{\alpha - 1} \right) \text{OPT.}$$

as claimed. To obtain the numerical constants, we optimize over $\alpha > 1$:

- In the worst case ($k_{\min} = 1$), the bound becomes $(2 + \frac{2}{\alpha-1})(3\alpha^2 + \alpha + \frac{\alpha}{\alpha-1})$. Minimizing this expression yields $\alpha = (7 + \sqrt{13})/6 \approx 1.7676$ and a value of $\frac{92+26\sqrt{13}}{3} \approx 61.9147$.
- In the large-memory regime ($k_{\min} \rightarrow \infty$), the bound reduces to $(2 + \frac{2}{\alpha-1})(\alpha^2 + \alpha + \frac{\alpha}{\alpha-1})$. Minimization gives $\alpha = 2$ and a value of 32.

This completes the proof of Theorem 2. \square

6. Conclusion and Future Directions

This work demonstrates that constant-competitive scheduling is achievable for LLM inference under dynamic KV-cache constraints, even without knowledge of response lengths. Our results suggest two broader insights. First, the staggered pipeline mechanism shows that *desynchronizing* job execution can be fundamentally more efficient than batching greedily (and thus simultaneously). Second, geometric slicing illustrates how disciplined preemption can tame non-clairvoyance: by accepting controlled overhead from periodic restarts, we avoid the unbounded delays that arise from prevalent heuristics.

We highlight several promising directions for future work. First, it would be valuable to explore more general models that incorporate online arrivals or heterogeneous prompt lengths. Our analysis focuses on the offline batch setting with identical prompt lengths. As discussed in Section 2.2, relaxing either assumption leads to strong hardness results. While recent works (e.g., Ao et al., 2025; Wang et al., 2025; Zhang et al., 2025b; Li et al., 2025b; Jaillet et al., 2025) have initiated the study of those extension models, it remains largely open to characterize which intermediate settings admit strong performance guarantees. Second, tightening the theoretical guarantees of our algorithms and establishing fundamental lower bounds is an important next step. Although we present the first constant competitive ratio for the non-clairvoyant setting, no non-trivial lower bounds are currently known. Proving such bounds—or further improving the upper bounds—would deepen our understanding of the inherent limits of non-clairvoyant scheduling under dynamic memory constraints. Third, extending our framework to multi-machine settings is a natural and practically relevant direction. Our model assumes a single GPU with a fixed KV-cache budget, whereas real-world LLM inference systems often distribute requests across multiple machines or GPUs with heterogeneous memory capacities. Developing algorithms that effectively route or migrate jobs in such environments poses significant new challenges and opportunities.

References

Anna Adamaszek, Tomasz Kociumaka, Marcin Pilipczuk, and Michał Pilipczuk. Hardness of approximation for strip packing. *ACM Trans. Comput. Theory*, 9(3):14:1–14:7, 2017. doi: 10.1145/3092026. URL <https://doi.org/10.1145/3092026>.

Ruicheng Ao, Gan Luo, David Simchi-Levi, and Xinshang Wang. Optimizing LLM inference: Fluid-guided online scheduling with memory constraints. *CoRR*, abs/2504.11320, 2025. doi: 10.48550/ARXIV.2504.11320. URL <https://doi.org/10.48550/arXiv.2504.11320>.

Baruch Awerbuch, Yossi Azar, Stefano Leonardi, and Oded Regev. Minimizing the flow time without migration. *SIAM J. Comput.*, 31(5):1370–1382, 2002. doi: 10.1137/S009753970037446X. URL <https://doi.org/10.1137/S009753970037446X>.

Yossi Azar, Stefano Leonardi, and Noam Touitou. Distortion-oblivious algorithms for minimizing flow time. In Joseph (Seffi) Naor and Niv Buchbinder, editors, *Proceedings of the 2022 ACM-SIAM Symposium on Discrete Algorithms, SODA 2022, Virtual Conference / Alexandria, VA, USA, January 9 - 12, 2022*, pages 252–274. SIAM, 2022. doi: 10.1137/1.9781611977073.13. URL <https://doi.org/10.1137/1.9781611977073.13>.

Luca Becchetti and Stefano Leonardi. Non-clairvoyant scheduling to minimize the average flow time on single and parallel machines. In Jeffrey Scott Vitter, Paul G. Spirakis, and Mihalis Yannakakis, editors, *Proceedings on 33rd Annual ACM Symposium on Theory of Computing, July 6-8, 2001, Heraklion, Crete, Greece*, pages 94–103. ACM, 2001. doi: 10.1145/380752.380782. URL <https://doi.org/10.1145/380752.380782>.

Luca Becchetti, Stefano Leonardi, Alberto Marchetti-Spaccamela, and Kirk Pruhs. Semi-clairvoyant scheduling. *Theor. Comput. Sci.*, 324(2-3):325–335, 2004. doi: 10.1016/J.TCS.2004.05.023. URL <https://doi.org/10.1016/j.tcs.2004.05.023>.

Ziyad Benomar and Vianney Perchet. Non-clairvoyant scheduling with partial predictions. In *Forty-first International Conference on Machine Learning, ICML 2024, Vienna, Austria, July 21-27, 2024*. OpenReview.net, 2024. URL <https://openreview.net/forum?id=jJLcXGB2uA>.

Ziyad Benomar, Romain Cosson, Alexander Lindermayr, and Jens Schlöter. Non-clairvoyant scheduling with progress bars. *CoRR*, abs/2509.19662, 2025. doi: 10.48550/ARXIV.2509.19662. URL <https://doi.org/10.48550/arXiv.2509.19662>.

Tom B. Brown, Benjamin Mann, Nick Ryder, Melanie Subbiah, Jared Kaplan, Prafulla Dhariwal, Arvind Neelakantan, Pranav Shyam, Girish Sastry, Amanda Askell, Sandhini Agarwal, Ariel Herbert-Voss, Gretchen Krueger, Tom Henighan, Rewon Child, Aditya Ramesh, Daniel M. Ziegler, Jeffrey Wu, Clemens Winter, Christopher Hesse, Mark Chen, Eric Sigler, Mateusz Litwin, Scott Gray, Benjamin Chess, Jack Clark, Christopher Berner, Sam McCandlish, Alec Radford, Ilya Sutskever, and Dario Amodei. Language models are few-shot learners. In Hugo Larochelle, Marc'Aurelio Ranzato, Raia Hadsell, Maria-Florina Balcan, and Hsuan-Tien Lin, editors, *Advances in Neural Information Processing Systems 33: Annual Conference on Neural Information Processing Systems 2020, NeurIPS 2020, December 6-12, 2020, virtual*, 2020. URL <https://proceedings.neurips.cc/paper/2020/hash/1457c0d6bfcb4967418bfb8ac142f64a-Abstract.html>.

Zixi Chen, Yinyu Ye, and Zijie Zhou. Adaptively robust LLM inference optimization under prediction uncertainty. *CoRR*, abs/2508.14544, 2025. doi: 10.48550/ARXIV.2508.14544. URL <https://doi.org/10.48550/arXiv.2508.14544>.

Esha Choukse, Pratyush Patel, Chaojie Zhang, Aashaka Shah, Íñigo Goiri, Saeed Maleki, Rodrigo Fonseca, and Ricardo Bianchini. Splitwise: Efficient generative LLM inference using phase splitting. *IEEE Micro*, 45(4):54–59, 2025. doi: 10.1109/MM.2025.3575361. URL <https://doi.org/10.1109/MM.2025.3575361>.

Leah Epstein and Rob van Stee. Lower bounds for on-line single-machine scheduling. *Theor. Comput. Sci.*, 299(1-3):439–450, 2003. doi: 10.1016/S0304-3975(02)00488-7. URL [https://doi.org/10.1016/S0304-3975\(02\)00488-7](https://doi.org/10.1016/S0304-3975(02)00488-7).

Leah Epstein, David S. Johnson, and Asaf Levin. Min-sum bin packing. *J. Comb. Optim.*, 36(2):508–531, 2018. doi: 10.1007/S10878-018-0310-X. URL <https://doi.org/10.1007/s10878-018-0310-x>.

Yichao Fu, Siqi Zhu, Runlong Su, Aurick Qiao, Ion Stoica, and Hao Zhang. Efficient LLM scheduling by learning to rank. In Amir Globersons, Lester Mackey, Danielle Belgrave, Angela Fan, Ulrich Paquet, Jakub M. Tomczak, and Cheng Zhang, editors, *Advances in Neural Information Processing Systems 38: Annual Conference on Neural Information Processing Systems 2024, NeurIPS 2024, Vancouver, BC, Canada, December 10 - 15, 2024*. URL http://papers.nips.cc/paper_files/paper/2024/hash/6c8985579293e0209bdaa4f21bb1d237-Abstract-Conference.html.

Yutong Geng, Enze Sun, Zonghan Yang, and Yuhao Zhang. Online flow time minimization: Tight bounds for non-preemptive algorithms. *CoRR*, abs/2511.03485, 2025. doi: 10.48550/ARXIV.2511.03485. URL <https://doi.org/10.48550/arXiv.2511.03485>.

Negin Golrezaei, Hamid Nazerzadeh, and Paat Rusmevichientong. Real-time optimization of personalized assortments. *Manag. Sci.*, 60(6):1532–1551, 2014. doi: 10.1287/MNSC.2014.1939. URL <https://doi.org/10.1287/mnsc.2014.1939>.

Google. Gemini api: Batch processing. <https://ai.google.dev/gemini-api/docs/batch-api>, 2024a. Accessed: December 29, 2025.

Google. Google gemini. <https://gemini.google.com/>, 2024b. Accessed: December 29, 2025.

Daya Guo, Dejian Yang, Haowei Zhang, Junxiao Song, Peiyi Wang, Qihao Zhu, Runxin Xu, Ruoyu Zhang, Shirong Ma, Xiao Bi, Xiaokang Zhang, Xingkai Yu, Yu Wu, Z. F. Wu, Zhibin Gou, Zhihong Shao, Zhuoshu Li, Ziyi Gao, Aixin Liu, Bing Xue, Bingxuan Wang, Bochao Wu, Bei Feng, Chengda Lu, Chenggang Zhao, Chengqi Deng, Chong Ruan, Damai Dai, Deli Chen, Dongjie Ji, Erhang Li, Fangyun Lin, Fucong Dai, Fuli Luo, Guangbo Hao, Guanting Chen, Guowei Li, H. Zhang, Hanwei Xu, Honghui Ding, Huazuo Gao, Hui Qu, Hui Li, Jianzhong Guo, Jiashi Li, Jingchang Chen, Jingyang Yuan, Jinhao Tu, Junjie Qiu, Junlong Li, J. L. Cai, Jiaqi Ni, Jian Liang, Jin Chen, Kai Dong, Kai Hu, Kaichao You, Kaige Gao, Kang Guan, Kexin Huang, Kuai Yu, Lean Wang, Lecong Zhang, Liang Zhao, Litong Wang, Liyue Zhang, Lei Xu, Leyi Xia, Mingchuan Zhang, Minghua Zhang, Minghui Tang, Mingxu Zhou, Meng Li, Miaojun Wang, Mingming Li, Ning Tian, Panpan Huang, Peng Zhang, Qiancheng Wang, Qinyu Chen, Qiushi Du, Ruiqi Ge, Ruisong Zhang, Ruizhe Pan, Runji Wang, R. J. Chen, R. L. Jin, Ruyi Chen, Shanghao Lu, Shangyan Zhou, Shanhua Chen, Shengfeng Ye, Shiyu Wang, Shuiping Yu, Shunfeng Zhou, Shuting Pan, S. S. Li, Shuang Zhou, Shaoqing Wu, Tao Yun, Tian Pei, Tianyu Sun, T. Wang, Wangding Zeng, Wen Liu, Wenfeng Liang, Wenjun Gao, Wenqin Yu, Wentao Zhang, W. L. Xiao, Wei An, Xiaodong Liu, Xiaohan Wang, Xiaokang Chen, Xiaotao Nie, Xin Cheng, Xin Liu, Xin Xie, Xingchao Liu, Xinyu Yang, Xinyuan Li, Xuecheng Su, Xuheng Lin, X. Q. Li, Xiangyue Jin, Xiaojin Shen, Xiaosha Chen, Xiaowen Sun, Xiaoxiang Wang, Xinnan Song, Xinyi Zhou, Xianzu Wang, Xinxia Shan, Y. K. Li, Y. Q. Wang, Y. X. Wei, Yang Zhang, Yanhong Xu, Yao Li, Yao Zhao, Yaofeng Sun, Yaohui Wang, Yi Yu, Yichao Zhang, Yifan Shi, Yiliang Xiong, Ying He, Yishi Piao, Yisong Wang, Yixuan Tan, Yiyang Ma, Yiyuan Liu, Yongqiang Guo, Yuan Ou, Yuduan Wang, Yue Gong, Yuheng Zou, Yujia He, Yunfan Xiong, Yuxiang Luo, Yuxiang You, Yuxuan Liu, Yuyang Zhou, Y. X. Zhu, Yanping Huang, Yaohui Li, Yi Zheng, Yuchen Zhu, Yunxian Ma, Ying Tang, Yukun Zha, Yuting Yan, Z. Z. Ren, Zehui Ren, Zhangli Sha, Zhe Fu, Zhean Xu, Zhenda Xie, Zhengyan Zhang, Zhewen Hao, Zhicheng Ma, Zhigang Yan, Zhiyu Wu, Zihui Gu, Zijia Zhu, Zijun Liu, Zilin Li, Ziwei Xie, Ziyang Song, Zizheng Pan, Zhen Huang, Zhipeng Xu, Zhongyu Zhang, and Zhen Zhang. Deepseek-r1 incentivizes reasoning in llms through reinforcement learning. *Nature*, 645(8081):633–638, September 2025. ISSN 1476-4687. doi: 10.1038/s41586-025-09422-z. URL <http://dx.doi.org/10.1038/s41586-025-09422-z>.

Zijian He, Reyna Abhyankar, Vikranth Srivatsa, and Yiying Zhang. Cognify: Supercharging gen-ai workflows with hierarchical autotuning. In Luiza Antonie, Jian Pei, Xiaohui Yu, Flavio Chierichetti, Hady W. Lauw, Yizhou Sun, and Srinivasan Parthasarathy, editors, *Proceedings of the 31st ACM SIGKDD Conference on Knowledge Discovery and Data Mining*, V.2, *KDD 2025, Toronto ON, Canada, August 3-7, 2025*, pages 932–943. ACM, 2025. doi: 10.1145/3711896.3736884. URL <https://doi.org/10.1145/3711896.3736884>.

Coleman Hooper, Sehoon Kim, Hiva Mohammadzadeh, Michael W. Mahoney, Yakun Sophia Shao, Kurt Keutzer, and Amir Ghodjami. Kvquant: Towards 10 million context length LLM inference with KV cache quantization. In Amir Globersons, Lester

Mackey, Danielle Belgrave, Angela Fan, Ulrich Paquet, Jakub M. Tomczak, and Cheng Zhang, editors, *Advances in Neural Information Processing Systems 38: Annual Conference on Neural Information Processing Systems 2024, NeurIPS 2024, Vancouver, BC, Canada, December 10 - 15, 2024*, 2024. URL http://papers.nips.cc/paper_files/paper/2024/hash/028fcbcf85435d39a40c4d61b42c99a4-Abstract-Conference.html.

Sungjin Im, Ravi Kumar, Mahshid Montazer Qaem, and Manish Purohit. Non-clairvoyant scheduling with predictions. *ACM Trans. Parallel Comput.*, 10(4):19:1–19:26, 2023. doi: 10.1145/3593969. URL <https://doi.org/10.1145/3593969>.

Aaron Jaech, Adam Kalai, Adam Lerer, Adam Richardson, Ahmed El-Kishky, Aiden Low, Alec Helyar, Aleksander Madry, Alex Beutel, Alex Carney, Alex Iftimie, Alex Karpenko, Alex Tachard Passos, Alexander Neitz, Alexander Prokofiev, Alexander Wei, Allison Tam, Ally Bennett, Ananya Kumar, Andre Saraiva, Andrea Vallone, Andrew Duberstein, Andrew Kondrich, Andrey Mishchenko, Andy Applebaum, Angela Jiang, Ashvin Nair, Barret Zoph, Behrooz Ghorbani, Ben Rossen, Benjamin Sokolowsky, Boaz Barak, Bob McGrew, Borys Minaiev, Botao Hao, Bowen Baker, Brandon Houghton, Brandon McKinzie, Brydon Eastman, Camillo Lugaressi, Cary Bassin, Cary Hudson, Chak Ming Li, Charles de Bourcy, Chelsea Voss, Chen Shen, Chong Zhang, Chris Koch, Chris Orsinger, Christopher Hesse, Claudia Fischer, Clive Chan, Dan Roberts, Daniel Kappler, Daniel Levy, Daniel Selsam, David Dohan, David Farhi, David Mely, David Robinson, Dimitris Tsipras, Doug Li, Dragos Oprica, Eben Freeman, Eddie Zhang, Edmund Wong, Elizabeth Proehl, Enoch Cheung, Eric Mitchell, Eric Wallace, Erik Ritter, Evan Mays, Fan Wang, Felipe Petroski Such, Filippo Raso, Florencia Leoni, Foivos Tsimpourlas, Francis Song, Fred von Lohmann, Freddie Sulit, Geoff Salmon, Giambattista Parascandolo, Gildas Chabot, Grace Zhao, Greg Brockman, Guillaume Leclerc, Hadi Salman, Haiming Bao, Hao Sheng, Hart Andrin, Hessam Bagherinezhad, Hongyu Ren, Hunter Lightman, Hyung Won Chung, Ian Kivlichan, Ian O’Connell, Ian Osband, Ignasi Clavera Gilaberte, and Ilge Akkaya. Openai o1 system card. *CoRR*, abs/2412.16720, 2024. doi: 10.48550/ARXIV.2412.16720. URL <https://doi.org/10.48550/arXiv.2412.16720>.

Sven Jäger, Guillaume Sagnol, Daniel Schmidt genannt Waldschmidt, and Philipp Warode. Competitive kill-and-restart and preemptive strategies for non-clairvoyant scheduling. *Math. Program.*, 210(1):457–509, 2025. doi: 10.1007/S10107-024-02118-8. URL <https://doi.org/10.1007/s10107-024-02118-8>.

Patrick Jaillet, Jiashuo Jiang, Konstantina Mellou, Marco Molinaro, Chara Podimata, and Zijie Zhou. Online Scheduling for LLM Inference with KV Cache Constraints. *CoRR*, abs/2502.07115, 2025. doi: 10.48550/ARXIV.2502.07115. URL <https://doi.org/10.48550/arXiv.2502.07115>.

Yunho Jin, Chun-Feng Wu, David Brooks, and Gu-Yeon Wei. S^3 : Increasing GPU utilization during generative inference for higher throughput. In Alice Oh, Tristan Naumann, Amir Globerson, Kate Saenko, Moritz Hardt, and Sergey Levine, editors, *Advances in Neural Information Processing Systems 36: Annual Conference on Neural Information Processing Systems 2023, NeurIPS 2023, New Orleans, LA, USA, December 10 - 16, 2023*, 2023. URL http://papers.nips.cc/paper_files/paper/2023/hash/3a13be0c5dae69e0f08065f113fb10b8-Abstract-Conference.html.

Bala Kalyanasundaram and Kirk R Pruhs. An optimal deterministic algorithm for online b-matching. *Theoretical Computer Science*, 233(1-2):319–325, 2000.

Woosuk Kwon, Zhuohan Li, Siyuan Zhuang, Ying Sheng, Lianmin Zheng, Cody Hao Yu, Joseph Gonzalez, Hao Zhang, and Ion Stoica. Efficient memory management for large language model serving with pagedattention. In Jason Flinn, Margo I. Seltzer, Peter Druschel, Antoine Kaufmann, and Jonathan Mace, editors, *Proceedings of the 29th Symposium on Operating Systems Principles, SOSP 2023, Koblenz, Germany, October 23-26, 2023*, pages 611–626. ACM, 2023. doi: 10.1145/3600006.3613165. URL <https://doi.org/10.1145/3600006.3613165>.

Stefano Leonardi and Danny Raz. Approximating total flow time on parallel machines. *J. Comput. Syst. Sci.*, 73(6):875–891, 2007. doi: 10.1016/J.JCSS.2006.10.018. URL <https://doi.org/10.1016/j.jcss.2006.10.018>.

Pengfei Li, Jianyi Yang, Mohammad A. Islam, and Shaolei Ren. Making AI less ‘thirsty’. *Commun. ACM*, 68(7):54–61, 2025a. doi: 10.1145/3724499. URL <https://doi.org/10.1145/3724499>.

Yueying Li, Jim Dai, and Tianyi Peng. Throughput-optimal scheduling algorithms for llm inference and ai agents. *arXiv preprint arXiv:2504.07347*, 2025b.

Andrea Lodi, Silvano Martello, and Michele Monaci. Two-dimensional packing problems: A survey. *Eur. J. Oper. Res.*, 141(2):241–252, 2002. doi: 10.1016/S0377-2217(02)00123-6. URL [https://doi.org/10.1016/S0377-2217\(02\)00123-6](https://doi.org/10.1016/S0377-2217(02)00123-6).

Sasha Luccioni, Yacine Jernite, and Emma Strubell. Power hungry processing: Watts driving the cost of AI deployment? In *The 2024 ACM Conference on Fairness, Accountability, and Transparency, FAccT 2024, Rio de Janeiro, Brazil, June 3-6, 2024*, pages 85–99. ACM, 2024. doi: 10.1145/3630106.3658542. URL <https://doi.org/10.1145/3630106.3658542>.

Will Ma and David Simchi-Levi. Algorithms for online matching, assortment, and pricing with tight weight-dependent competitive ratios. *Operations Research*, 68(6):1787–1803, 2020.

Aranyak Mehta, Amin Saberi, Umesh V. Vazirani, and Vijay V. Vazirani. Adwords and generalized online matching. *J. ACM*, 54(5):22, 2007. doi: 10.1145/1284320.1284321. URL <https://doi.org/10.1145/1284320.1284321>.

Microsoft. Microsoft copilot. <https://copilot.microsoft.com/>, 2023. Accessed: December 29, 2025.

Rajeev Motwani, Steven Phillips, and Eric Torng. Nonclairvoyant scheduling. *Theoretical Computer Science*, 130(1):17–47, 1994. ISSN 0304-3975. doi: [https://doi.org/10.1016/0304-3975\(94\)90151-1](https://doi.org/10.1016/0304-3975(94)90151-1). URL <https://www.sciencedirect.com/science/article/pii/0304397594901511>.

NVIDIA. Tensorrt-llm: A tensorrt toolbox for optimized large language model inference. <https://github.com/NVIDIA/TensorRT-LLM>, 2023. Open-source library for optimizing LLM inference on NVIDIA GPUs; includes state-of-the-art optimizations and a Python API.

OpenAI. GPT-4 technical report, 2023. URL <https://doi.org/10.48550/arXiv.2303.08774>.

OpenAI. Batch api guide. <https://platform.openai.com/docs/guides/batch>, 2024. Accessed: December 29, 2025.

Zaifeng Pan, AJJKUMAR PATEL, Yipeng Shen, Zhengding Hu, Yue Guan, Wan-Lu Li, Lianhui Qin, Yida Wang, and Yufei Ding. KVFlow: Efficient prefix caching for accelerating LLM-based multi-agent workflows. In *The Thirty-ninth Annual Conference on Neural Information Processing Systems*, 2025. URL <https://openreview.net/forum?id=5Iw1nDtYmT>.

Emma Strubell, Ananya Ganesh, and Andrew McCallum. Energy and policy considerations for deep learning in NLP. In Anna Korhonen, David R. Traum, and Lluís Màrquez, editors, *Proceedings of the 57th Conference of the Association for Computational Linguistics, ACL 2019, Florence, Italy, July 28- August 2, 2019, Volume 1: Long Papers*, pages 3645–3650. Association for Computational Linguistics, 2019. doi: 10.18653/V1/P19-1355. URL <https://doi.org/10.18653/v1/p19-1355>.

Ashish Vaswani, Noam Shazeer, Niki Parmar, Jakob Uszkoreit, Llion Jones, Aidan N. Gomez, Łukasz Kaiser, and Illia Polosukhin. Attention is all you need. In *Advances in Neural Information Processing Systems 30*, pages 5998–6008, 2017. URL https://proceedings.neurips.cc/paper_files/paper/2017/file/3f5ee243547dee91fb053c1c4a845aa-Paper.pdf.

Meixuan Wang, Yinyu Ye, and Zijie Zhou. Llm serving optimization with variable prefill and decode lengths. *arXiv preprint arXiv:2508.06133*, 2025.

Jason Wei, Xuezhi Wang, Dale Schuurmans, Maarten Bosma, Brian Ichter, Fei Xia, Ed H. Chi, Quoc V. Le, and Denny Zhou. Chain-of-thought prompting elicits reasoning in large language models. In Sanmi Koyejo, S. Mohamed, A. Agarwal, Danielle Belgrave, K. Cho, and A. Oh, editors, *Advances in Neural Information Processing Systems 35: Annual Conference on Neural Information Processing Systems 2022, NeurIPS 2022, New Orleans, LA, USA, November 28 - December 9, 2022*, 2022. URL http://papers.nips.cc/paper_files/paper/2022/hash/9d5609613524ecf4f15af0f7b31abca4-Abstract-Conference.html.

Jiayi Zhang, Jinyu Xiang, Zhaoyang Yu, Fengwei Teng, Xionghui Chen, Jiaqi Chen, Mingchen Zhuge, Xin Cheng, Sirui Hong, Jinlin Wang, Bingnan Zheng, Bang Liu, Yuyu Luo, and Chenglin Wu. Aflow: Automating agentic workflow generation. In *The Thirteenth International Conference on Learning Representations, ICLR 2025, Singapore, April 24-28, 2025*. OpenReview.net, 2025a. URL <https://openreview.net/forum?id=z5uVAKwmjf>.

Wenxin Zhang, Yueying Li, Ciamac C Moallemi, and Tianyi Peng. Tail-optimized caching for llm inference. *arXiv preprint arXiv:2510.15152*, 2025b.

Lianmin Zheng, Wei-Lin Chiang, Ying Sheng, Tianle Li, Siyuan Zhuang, Zhanghao Wu, Yonghao Zhuang, Zhuohan Li, Zi Lin, Eric P. Xing, Joseph E. Gonzalez, Ion Stoica, and Hao Zhang. Lmsys-chat-1m: A large-scale real-world LLM conversation dataset. In *The Twelfth International Conference on Learning Representations, ICLR 2024, Vienna, Austria, May 7-11, 2024*. OpenReview.net, 2024a. URL <https://openreview.net/forum?id=BOfDKxfwt0>.

Lianmin Zheng, Liangsheng Yin, Zhiqiang Xie, Chuyue Sun, Jeff Huang, Cody Hao Yu, Shiyi Cao, Christos Kozyrakis, Ion Stoica, Joseph E. Gonzalez, Clark W. Barrett, and Ying Sheng. Sglang: Efficient execution of structured language model programs. In Amir Globersons, Lester Mackey, Danielle Belgrave, Angela Fan, Ulrich Paquet, Jakub M. Tomczak, and Cheng Zhang, editors, *Advances in Neural Information Processing Systems 38: Annual Conference on Neural Information Processing Systems 2024, NeurIPS 2024, Vancouver, BC, Canada, December 10 - 15, 2024*, 2024b. URL http://papers.nips.cc/paper_files/paper/2024/hash/724be4472168f31ba1c9ac630f15dec8-Abstract-Conference.html.

Zangwei Zheng, Xiaozhe Ren, Fuzhao Xue, Yang Luo, Xin Jiang, and Yang You. Response length perception and sequence scheduling: An llm-empowered LLM inference pipeline. In Alice Oh, Tristan Naumann, Amir Globerson, Kate Saenko, Moritz Hardt, and Sergey Levine, editors, *Advances in Neural Information Processing Systems 36: Annual Conference on Neural Information Processing Systems 2023, NeurIPS 2023, New Orleans, LA, USA, December 10 - 16, 2023*, 2023. URL http://papers.nips.cc/paper_files/paper/2023/hash/ce7ff3405c782f761fac7f849b41ae9a-Abstract-Conference.html.

Yinmin Zhong, Shengyu Liu, Junda Chen, Jianbo Hu, Yibo Zhu, Xuanzhe Liu, Xin Jin, and Hao Zhang. Distserve: Disaggregating prefill and decoding for goodput-optimized large language model serving. In Ada Gavrilovska and Douglas B. Terry, editors, *18th USENIX Symposium on Operating Systems Design and Implementation, OSDI 2024, Santa Clara, CA, USA, July 10-12, 2024*, pages 193–210. USENIX Association, 2024. URL <https://www.usenix.org/conference/osdi24/presentation/zhong-yinmin>.

This page is intentionally blank. The e-companion (EC) starts next page.

EC.1. Numerical Experiments

We evaluate the performance of our proposed algorithms using a discrete-time event simulator that faithfully captures the memory-constrained scheduling dynamics defined in Section 2. Our evaluation is designed to bridge the gap between theoretical analysis and practical deployment, answering two key questions:

1. Do the structural benefits of geometric scheduling observed in our worst-case analysis hold in controlled settings?
2. Can these insights translate into tangible performance gains under realistic, heavy-tailed LLM workloads?

To this end, we organize our experiments into two categories:

Theoretical-Concept Experiments (Section EC.1.2). We first deploy small-scale synthetic workloads to isolate key structural properties of the algorithms. These micro-benchmarks serve to validate our theoretical insights—specifically, the ability of staggered starts to smooth memory usage and the robustness of kill-and-restart policies under adversarial conditions—in a controlled environment free from the noise of random distributions.

Trace-Driven Experiments (Section EC.1.3). We then evaluate practical performance using realistic job traces derived from the LMSYS-Chat-1M dataset (Zheng et al., 2024a). These macro-benchmarks demonstrate the effectiveness of our algorithms and their heuristic variants in handling the right-skewed generation lengths characteristic of modern LLM inference.

EC.1.1. Baselines

We first introduce the baseline policies considered in our numerical experiments.

Baselines from Prior Work. We use two baselines from prior work for comparison.

- MC-SF (Memory-Constrained Shortest First) from (Jaillet et al., 2025): a clairvoyant greedy algorithm that employs shortest job first scheduling under memory constraints, admitting as many jobs as possible in order of increasing response length.
- A-MIN from (Chen et al., 2025), a non-clairvoyant algorithm that maintains an estimate \tilde{o}_i of response lengths o_i based on observed progress, prioritizes jobs with the smallest estimated sizes, and kills the job with minimum estimated remaining length when memory is not sufficient. It also admits as many jobs as possible in order of increasing estimated response length, breaking tie uniformly at random.

Practical Baseline. We implement a practical baseline vLLM similar to the default vLLM scheduler (Kwon et al., 2023), which describes a family of First-Come-First-Served (FCFS) policy: jobs are admitted in order of arrival¹⁵, and when memory is insufficient, the job with the latest arrival time is evicted to free memory. This ensures fairness among jobs and achieves good average latency in practice.

¹⁵ In our model, all jobs arrive at time 0. Thus, jobs are ordered by their indices by default.

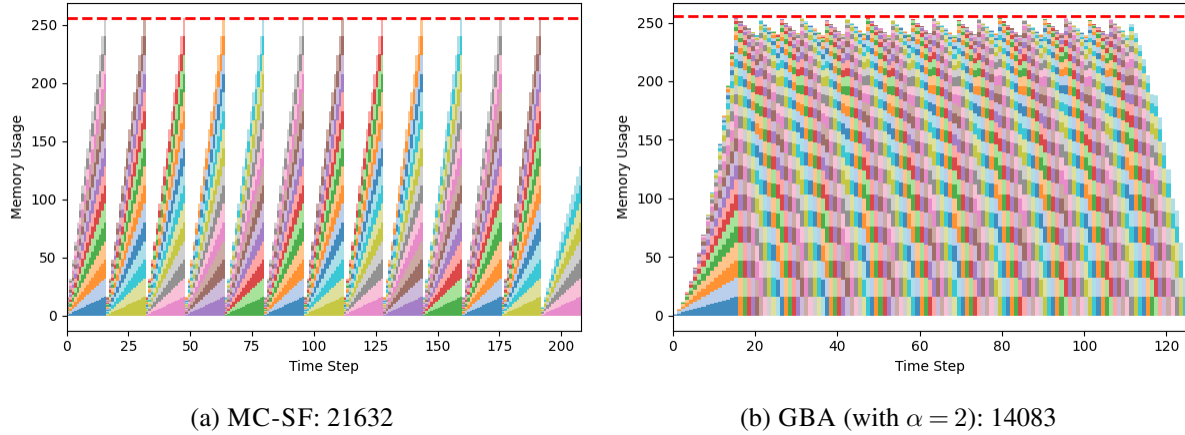


Figure EC.1 Uniform-size distribution results for clairvoyant algorithms. The total flow times are indicated in the titles. The x -axis represents time (rounds), and the y -axis represents the usage of memory in each round, where each job is represented by a colored block.

In our simulator we remove production safeguards (e.g., watermark mechanisms for memory overflow), making it slightly more aggressive; this can only improve its performance in our setting.

EC.1.2. Theoretical-Concept Experiments

In this section, we present our two theoretical-concept experiments.

Uniform-Size Distribution for Clairvoyant Algorithms. We simulate a workload of $n = 200$ jobs, each having identical response length $o_i = 16$ and prompt length $s = 0$, under a memory budget of $M = 256$.

As illustrative in Figure EC.1, MC-SF exhibits synchronized execution waves that repeatedly reach the memory capacity, leading to inefficient resource utilization. In contrast, GBA staggers job start times, maintaining a smoother and more uniform memory profile over time.

Two-Point Distribution for Non-Clairvoyant Algorithms. We consider an instance where all jobs share a prompt length of $s = 96$. The response lengths follow a bimodal distribution: six “long” jobs have $o_i = 160$, while the remaining 194 “short” jobs have $o_i = 1$. The memory budget is fixed at $M = 256$.

The results in Figure EC.2 reveal severe head-of-line blocking in both vLLM and A-MIN. GSA, however, mitigates this by strategically killing long jobs to admit short ones, thereby preventing prolonged blocking phases. Notably, the randomized strategy of A-MIN yields no significant improvement in this adversarial setting, as it still fall into the “let-long-jobs-finish” trap.

EC.1.3. Trace-Driven Experiments

To capture real-world job size distributions, we construct workloads using token counts from the LMSYS-Chat-1M dataset (Zheng et al., 2024a). Specifically, the job response length o_i is defined as the number of tokens in the first assistant response of each conversation. The prompt length is set to $s = 79$, reflecting the

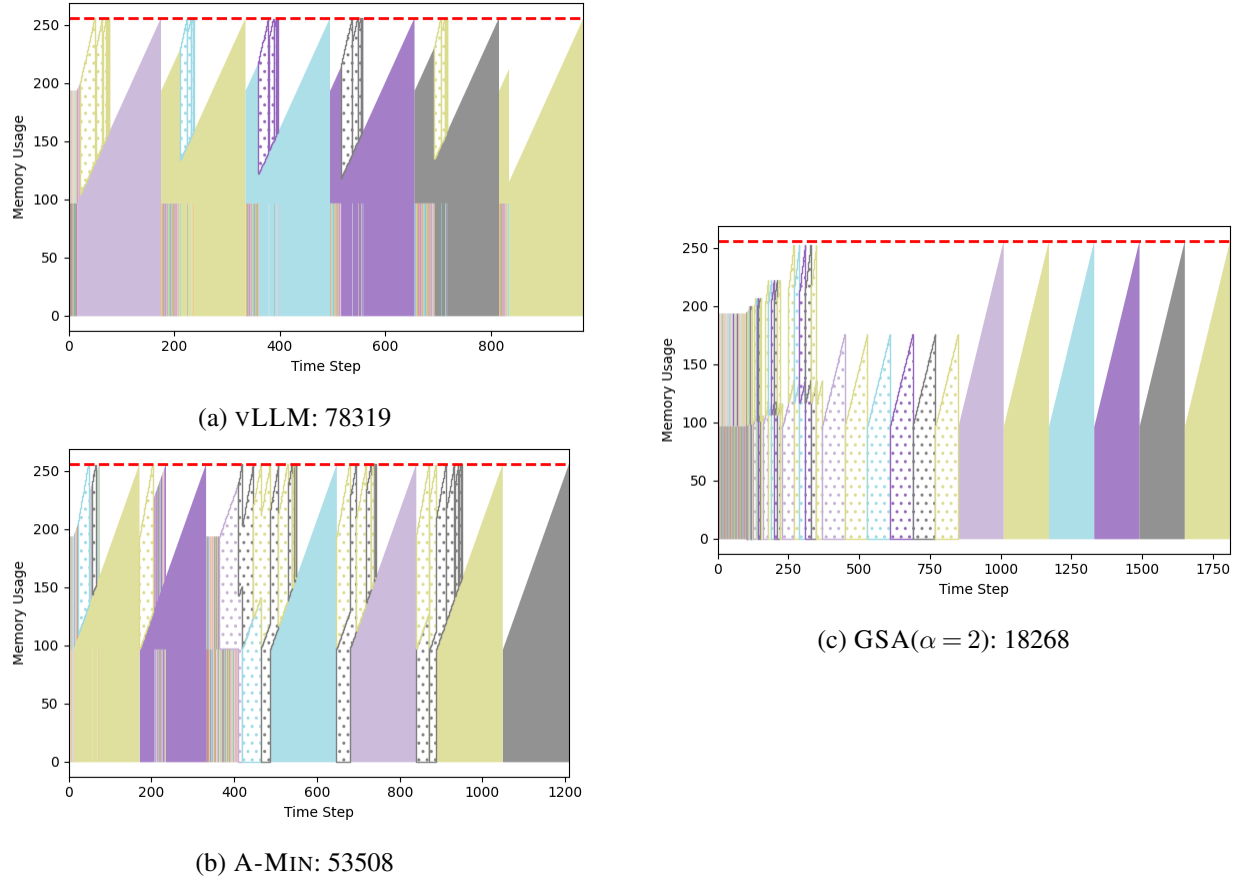


Figure EC.2 Two-point distribution results for non-clairvoyant algorithms. The total flow times are indicated in the titles. The x -axis represents time (rounds), and the y -axis represents the usage of memory in each round, where each finished job is represented by a colored block, and each killed job is represented by a dotted block.

average token count of user messages preceding the response. Figure EC.3 illustrates the resulting response length distribution, which exhibits the right-skewed characteristic typical of LLM inference workloads. For each trial with n jobs used in the simulation, the first n valid rows in the dataset are selected.

Due to the right-skewed job size distributions observed in real-world LLM inference workloads, directly implementing GBA and GSA may lead to suboptimal memory utilization and increased idle times: while fixed, geometrically rounded slice lengths ensure clean theoretical guarantees, in practice most jobs exit before the slice completes and the pipeline remains idle until the slice ends. To address this, we implement two practical variants of our algorithms for trace-driven experiments while retaining their worst-case approximation / competitiveness guarantees.

Dynamic Refill (GBA-D). Our theoretical algorithm GBA utilizes geometric slicing to simplify analysis. While this bridges the analysis from clairvoyant to non-clairvoyant settings, the synchronous rounds and fixed slice lengths are practically inefficient and can be improved by taking simple heuristics to eliminate the deliberate synchronization. GBA-D, our heuristic variant of GBA, employs a *dynamic refill* strategy:

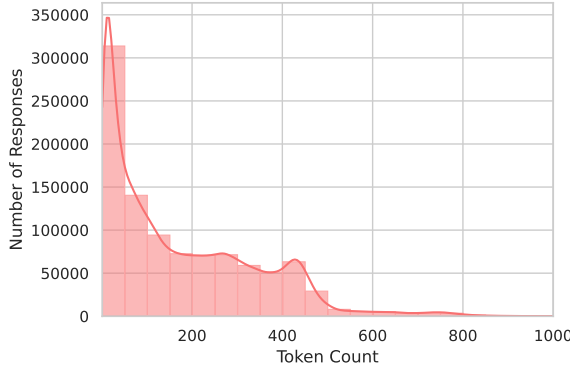


Figure EC.3 Response length distribution from the LMSYS-Chat-1M dataset, counted using `c1100k_base`, the tokenizer of GPT-4 (OpenAI, 2023).

- Whenever it is possible to continue the pipeline with a slice length equal to the smallest unfinished job response length ($\tau = o_i$) without violating memory feasibility, it admits the job immediately.

GBA-D never delays any job relative to the baseline GBA schedule; it only fills idle time, and therefore preserves the worst-case guarantee. In our experiments, GBA-D achieves the best performance on nearly all instances.

Speculative Runs (GSA-SPEC). In the non-clairvoyant setting, we must pessimistically choose the slice length to ensure memory feasibility. However, this may lead to under-utilization of memory due to not fully utilize the available budget. To mitigate this, GSA-SPEC, our heuristic variant of GSA, further enhances dynamic refill with *speculative runs*.

- When the memory is available after admitting all jobs in the current pipeline, it opportunistically starts new speculative runs for unfinished jobs using the freed memory.
- When the memory is insufficient, it kills the speculative jobs to ensure the original geometric slicing schedule is maintained.
- The speculative runs are started and killed in a First-Come-First-Serve (FCFS) manner like vLLM.

This heuristic further improves memory utilization by utilizing freed memory for speculative runs, while maintaining the theoretical guarantees of GSA.

Trace-Driven Power-of-Two Rounding Results. We begin by evaluating performance using a *power-of-two quantized* workload where response lengths are rounded up to the nearest power of two. This setting serves two purposes. First, from a systems perspective, it mirrors the behavior of memory allocators commonly used in OS and GPU runtimes, where resource reservations effectively snap to power-of-two boundaries to minimize external fragmentation. Second, from an algorithmic perspective, it aligns the workload granularity with the geometric phase structure of GSA. This allows us to isolate the core efficiency of our scheduling logic by reducing the noise from fine-grained size variations, effectively testing the algorithm

under a “structured uncertainty” regime while retaining practical relevance. In Figure EC.4, we present the mean flow times—a metric that is linearly related to total flow time, but more interpretable with growing n —under memory budgets $M \in \{4096, 8192\}$, and vary n from 100 to 1000. GBA-D consistently outperforms all baselines, and GSA-SPEC also demonstrates competitive performance, steadily surpassing vLLM and A-MIN. Notably, as n increases, the performance gap between our proposed algorithms and the baselines widens, highlighting their scalability and effectiveness in handling larger workloads.

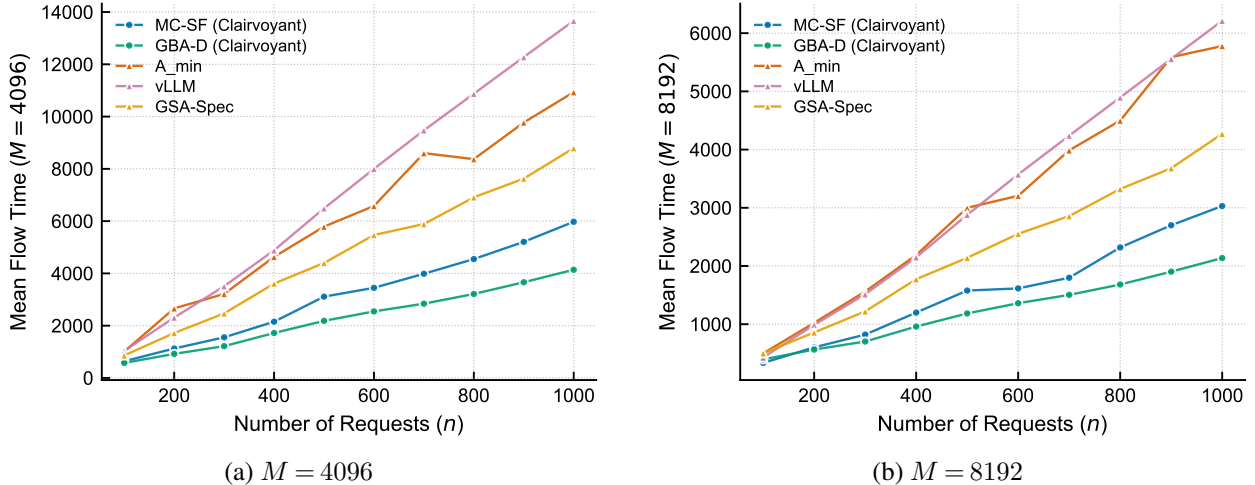


Figure EC.4 Results of trace-driven power-of-two rounding experiments. Each panel shows mean flow time—total flow time divided by n —as we sweep n under a fixed memory budget. GSA-SPEC uses $\alpha = 2$ and $\beta = 64$.

Trace-driven Experiments Results. In Figure EC.5, we present mean flow times under memory budgets $M \in \{4096, 8192\}$, varying n from 100 to 1000, without any rounding of job sizes.

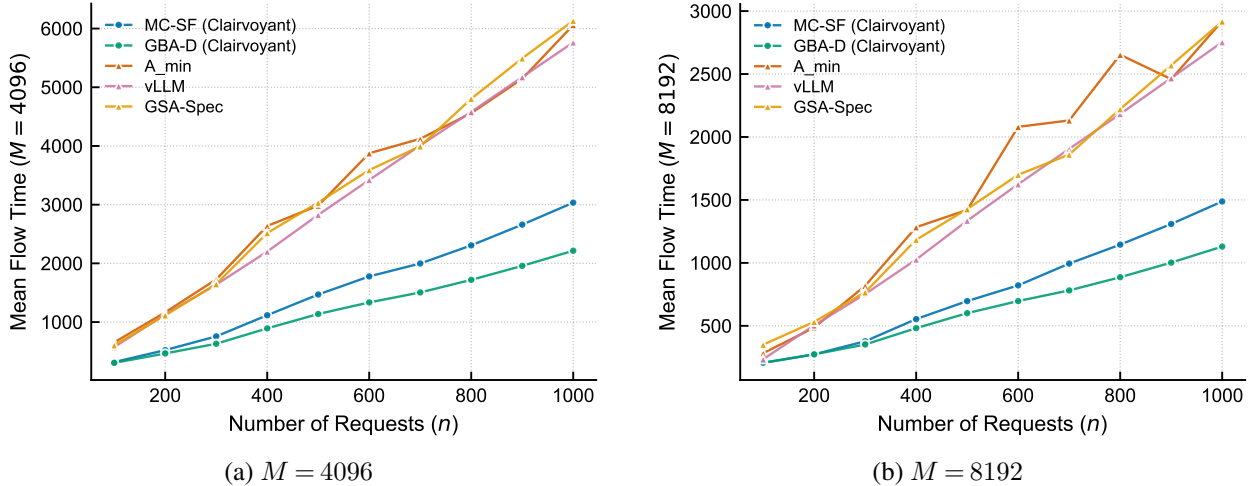


Figure EC.5 Results of trace-driven experiments. Each panel shows mean flow time—total flow time divided by n —as we sweep n under a fixed memory budget. GSA-SPEC uses $\alpha = 2$ and $\beta = 256$.

In these trace-driven settings, GBA-D continues to demonstrate superior performance, and GSA-SPEC remains competitive with the baselines. Comparing these results with the power-of-two experiments suggests that the increased challenge for GSA-SPEC stems from memory under-utilization, a consequence of using conservative slice lengths for diverse job sizes. However, by allowing speculative runs and tuning parameters like β , GSA-SPEC can better adapt to the workload characteristics, improving memory utilization and achieving a favorable balance between theoretical guarantees and practical performance.

EC.2. Missing Proofs in Section 3.1

EC.2.1. Proof of the Approximation Ratio of 2 in Theorem 1

In this section, we present the formal proof of the approximation ratio of 2 stated in Theorem 1.

Proof of approximation ratio of 2 in Theorem 1. Let $L \triangleq \lceil \tau/2 \rceil$. We first establish a necessary condition for feasibility: in any memory-valid schedule where S_i and C_i denote the start and completion times of job i (indexed $0, 1, \dots$), the start times $S_0 \leq S_1 \leq \dots$ must satisfy

$$S_{i+k} - S_i \geq L \quad \text{for all } i. \quad (\text{EC.1})$$

To prove this, assume for the sake of contradiction that $S_{i+k} - S_i \leq L - 1$ for some i . Consider the system state at time $T \triangleq S_i + \tau - 1$. At this time, job i is in its final round of execution ($u_{i,T} = \tau - 1$) and consumes $s + \tau$ memory. Since $S_{i+r} \leq S_{i+k} \leq S_i + L - 1$ for all $r \in \{1, \dots, k\}$, the progress of job $i+r$ at time T satisfies:

$$u_{i+r,T} = T - S_{i+r} \geq (S_i + \tau - 1) - (S_i + L - 1) = \tau - L.$$

Consequently, each of these k jobs consumes at least $s + (\tau - L) + 1 = s + \lfloor \tau/2 \rfloor + 1$ memory. Summing over the window of $k + 1$ jobs $(i, i + 1, \dots, i + k)$, the total memory usage at time T is:

$$\mathbf{Mem}(T) \geq (s + \tau) + k \left(s + \left\lfloor \frac{\tau}{2} \right\rfloor + 1 \right) = (k + 1)s + \tau + k + k \left\lfloor \frac{\tau}{2} \right\rfloor.$$

Using the inequality $\lfloor x/2 \rfloor \geq (x - 1)/2$, we have $\lfloor \tau/2 \rfloor \geq (\tau - 1)/2$. Substituting this bound:

$$\mathbf{Mem}(T) \geq (k + 1)s + \tau + k + \frac{k(\tau - 1)}{2} = (k + 1)s + \frac{\tau(k + 1) + \tau + k}{2}.$$

Comparing this with the definition of peak memory in Lemma 1:

$$\mathbf{Peak}(k + 1, \tau, s) = (k + 1)s + \frac{\tau(k + 1) + \tau + (k + 1) - \gcd(k + 1, \tau)}{2}.$$

Since $\gcd(k + 1, \tau) \geq 1$, we have $(k + 1) - \gcd(k + 1, \tau) \leq k$. Therefore:

$$\mathbf{Mem}(T) \geq \mathbf{Peak}(k + 1, \tau, s).$$

By definition of k , $\text{Peak}(k+1, \tau, s) > M$. This implies $\text{Mem}(T) > M$, yielding the contradiction to memory feasibility. Thus (EC.1) holds.

We now continue to the approximation ratio. By (EC.1), any group of k jobs in the optimal schedule takes at least L rounds to admit, i.e., $S_i^{\text{OPT}} \geq \lfloor i/k \rfloor L$, and

$$C_i^{\text{OPT}} \geq \left\lfloor \frac{i}{k} \right\rfloor L + \tau.$$

In our algorithm (SPS), the completion time of job i is:

$$C_i^{\text{SPS}} = \left\lfloor \frac{i\tau}{k} \right\rfloor + \tau.$$

Using the inequality $\lfloor i\tau/k \rfloor < (\lfloor i/k \rfloor + 1)\tau$ and $2L \geq \tau$:

$$C_i^{\text{SPS}} < \left(\left\lfloor \frac{i}{k} \right\rfloor + 1 \right) \tau + \tau = \left(\left\lfloor \frac{i}{k} \right\rfloor + 2 \right) \tau \leq 2 \left(\left\lfloor \frac{i}{k} \right\rfloor L + \tau \right) \leq 2C_i^{\text{OPT}}.$$

Thus, $C_i^{\text{SPS}} \leq 2C_i^{\text{OPT}}$ for all i , completing the proof. \square

REMARK EC.1. Our analysis of approximation ratio of 2 in Theorem 1 above relies on a rigid structural property, the spacing lower bound in (EC.1), of the optimal schedule. This is unique to the identical-job setting. For general instances, OPT can exhibit more complex behavior, ruling out such simple structural comparisons.

EC.2.2. Lower Bounds for SIMULTANEOUS-SCHEDULE

We first restate the SIMULTANEOUS-SCHEDULE (SIMS) used in Section 3.1, with more details. For identical jobs with prompt length s and response length o , SIMS admits jobs in batches of size

$$B \triangleq \left\lfloor \frac{M}{s+o} \right\rfloor,$$

runs each batch for o rounds, and starts a new batch only after the current batch finishes. All jobs in the same batch complete simultaneously. This procedure describes the behavior of a family of greedy algorithms when M is a multiple of $s+o$.

In the following, we use ε to denote $o(1)$, a small positive constant that can be arbitrarily close to 0 in the asymptotic regime, to avoid confusion with response length o .

PROPOSITION EC.1 (Asymptotic lower bound of 2 for SIMS). *There exists a family of identical-job instances such that the approximation ratio of SIMS is at least $2 - \varepsilon$ even in the asymptotic regime where $M \rightarrow \infty$, $n \rightarrow \infty$, and $M = o(n)$.*

Proof. Fix $s = 0$ and let the response length o grow with M , so that both $o \rightarrow \infty$ and $B \triangleq M/o \rightarrow \infty$ are integers. Consider n jobs with n a multiple of B . SIMS completes batches of size B every o rounds, so the total flow time is

$$\text{FLOWTIME[SIMS]} = Bo \sum_{j=1}^{n/B} j = \frac{on^2}{2B} + O(no).$$

On the other hand, by Lemma 2 with $\tau = o$ and $s = 0$, the maximum feasible parallelism for a staggered schedule satisfies

$$k^*(\tau, s) \geq \left\lfloor \frac{2M - o + 1}{o + 1} \right\rfloor = \left\lfloor 2B - \frac{2B - 1}{o + 1} \right\rfloor.$$

Let $k \triangleq k^*(\tau, s)$ and consider SPS with $(k, \tau) = (k, o)$. Using the standard bound on its total flow time,

$$\text{FLOWTIME[SPS]} \leq no + \frac{o}{2k} n(n-1) = \frac{on^2}{2k} + O(no).$$

Since $\text{OPT} \leq \text{FLOWTIME[SPS]}$, we obtain

$$\frac{\text{FLOWTIME[SIMS]}}{\text{OPT}} \geq \frac{\text{FLOWTIME[SIMS]}}{\text{FLOWTIME[SPS]}} \geq \frac{k}{B} \cdot (1 - \varepsilon) \geq \left(2 - \frac{2}{o+1} - \varepsilon\right).$$

Letting $o \rightarrow \infty$ yields the desired ratio. \square

PROPOSITION EC.2 (Lower bound approaching 3 for SIMS). *There exists a family of identical-job instances for which the approximation ratio of SIMS approaches 3 from below.*

Proof. Fix $s = 0$ and let o be a large multiple of 3. Choose an integer $\delta \geq 2$ and define a start-time spacing

$$d \triangleq \frac{o}{3} + \delta.$$

Set the memory budget to

$$M \triangleq 3o - 3d + 3 = 2o - 3\delta + 3,$$

so $M < 2o$ and SIMS admits only one job at a time, i.e., $B = 1$. Thus

$$\text{FLOWTIME[SIMS]} = \frac{on(n+1)}{2}.$$

Now consider the staggered schedule, \mathcal{S} , that starts job i at time id and runs it for o rounds. Because $d > o/3$, at most three jobs overlap at any time. The peak memory usage occurs when the oldest active job is about to finish, at which time the progress values of the three jobs are at most o , $o - d$, and $o - 2d$. The total memory usage is therefore at most

$$o + (o - d) + (o - 2d) + 3 = 3o - 3d + 3 = M,$$

so the schedule is feasible. Its total flow time is

$$\text{FLOWTIME}[\mathcal{S}] = no + d \cdot \frac{n(n-1)}{2}.$$

Consequently,

$$\frac{\text{FLOWTIME}[\text{SIMS}]}{\text{OPT}} \geq \frac{\text{FLOWTIME}[\text{SIMS}]}{\text{FLOWTIME}[\mathcal{S}]} \geq \frac{o}{d} \cdot (1 - \varepsilon) = \frac{3}{1 + 3\delta/o} \cdot (1 - \varepsilon).$$

Letting $o \rightarrow \infty$ with fixed δ shows that the ratio approaches 3 from below. \square

REMARK EC.2. The instance construction in Proposition EC.2 corresponds to the worst-case scenario in the 4-approximation analysis of SIMS for identical jobs by Jaillet et al. (2025). Regarding the memory-area bound, the average per-round memory usage of SIMS approaches $M/4$ when M is slightly less than $2o$, implying an approximation guarantee of nearly 4. However, in this specific scenario, OPT is also unable to fully utilize the available memory (e.g., because the spacing constraint (EC.1) prevents perfect packing of triangular memory profiles); consequently, the actual approximation ratio approaches 3 rather than 4, leaving a gap between the upper and lower bounds for SIMS on identical-job instances.